EXAMENSARBETE

Frequency analysis of accelerometer measurements on trains

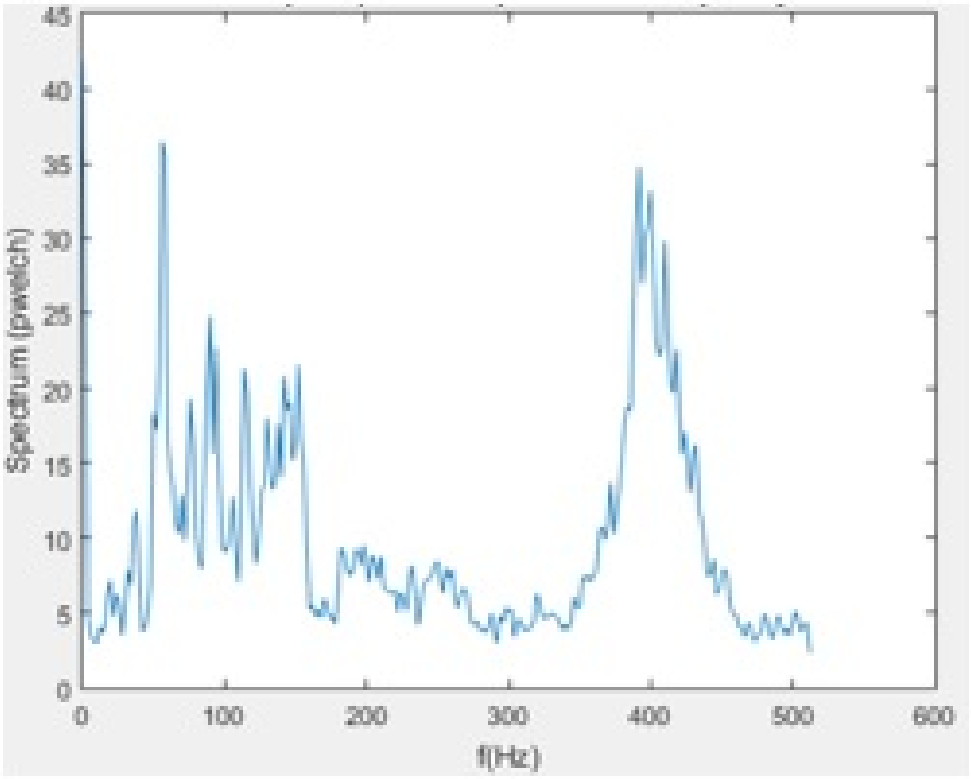

Jonas Majala

Civilingenjör, Väg- och vattenbyggnad
2017

Luleå tekniska universitet
Institutionen för samhällsbyggnad och naturresurser

LULEÅ TEKNISKA UNIVERSITET

Acknowledgements

As an end to the master programme studies in civil engineering at Luleå Technical University with specialization in soil and rock mechanics, a deeper study into the geotechnical field has been performed, which is compiled in this master thesis.

The subject for this study is frequency analysis of accelerometer acceleration measurements performed on trains. This study is done in cooperation with Luleå Technical University and Trafikverket, with the initiative from Prof. Jan Laue.

Therefore, I will start with giving thanks to my supervisor and examiner Prof. Jan Laue who gave me the opportunity to work with this subject in soil dynamics.

I want to thank all I have been in contact with at Trafikverket who has made an excellent job to help me with getting needed information and data for the study. I especially want to thank Erik Eriksson who has provided me with geotechnical information and Dr. Arne Nissen who provided me with the accelerometer measurement data.

I want to give great thanks to Associate Prof. Niklas Grip at the Department of Engineering Sciences and Mathematics, who help me with Matlab coding to ensure that the transformation of measurement data would be correct.

I want to thank my colleague Carlos Rojas, who has been a great support and help with my work on the thesis.

Finally, I want to thank friends and family who has through the whole time of my studies supported and encouraged me to continue until I reach the goal.

Luleå in May 2017

Jonas Majala

Sammanfattning

Då trafiklasterna längs Malmbanan har ökat med åren, samt att det idag finns önskemål från LKAB att ytterligare öka tonnaget på malmvagnarna. Så har detta skapat problem i järnvägsöverbyggnaden och att detta medför utmaningar till att kunna öka trafiklasterna ytterligare. För att kunna hitta lösningar till att få en mer bärkraftig järnvägsöverbyggnad, som klarar av dessa höga trafiklaster som dessutom skapar höga dynamiska laster på grund av längden på tågen. Behövs förståelse för vad som sker i de underliggande jordmaterialen när de blir utsatta för dynamiska laster. Därmed är frekvensanalys av accelerationsmätningar från accelerometrar en möjlig metod för analys av dynamiska lasters påverkan på underliggande jordmaterial. Vilket ger kunskap om vilka jordmaterial som blir utsatta för resonans på grund av vibrationerna från tågen och vilka möjliga problem detta kan medföra.

För analysen har två olika sträckningar längs bandel 118 valts ut. Nämligen sträckning Tolikberget km 1222–1223 där Trafikverket har påtalat att problem finns i järnvägsöverbyggnaden. Samt en referenssträcka där det bör vara goda möjligheter att kunna verifiera att metoden ger ett tillförlitligt resultat. Denna sträckning är Polcirkeln-Koskivaara km 1250+500–1251+600, som domineras av ett myrområde där undergrunden består till stora djup av torv, vilket är en fördel då det endast består av en typ av jordmaterial.

Dessutom har mätningar analyserats från stationära accelerometrar från Notviken, vilka monterats på sliper respektive räl. Därmed har en jämförelse utförts mellan stationära mätningars resultat och de mätresultat som är utförda med tåg vid Tolikberget och Polcirkeln-Koskivaara. Vilket visar att det är möjligt att utföra mätningar på båda sätten för att få önskvärd information om jordens och de andra komponenternas beteende under dynamisk belastning.

Från analysen av de utvalda sträckningarna vid Tolikberget och Polcirkeln-Koskivaara framgår att resultaten korrelerar väl med de förväntade värdena från handberäkningarna. Vilket bekräftar att metoden kan ses som tillförlitlig samt användbar för fortsatta analyser.

Den mest kritiska konsekvensen som kan uppstå vid resonans av jordlagren i undergrunden vid sträckningen i Tolikberget och Polcirkeln-Koskivaara, är förvätskning av jorden. Vilket genom analys kunde bekräftas vara möjligt. Detta skulle medföra att undergrunden tappar sin bärförmåga vilket skulle leda till oönskade sättningar. Samt att en risk finns för att vattentrycket i undergrunden blir så hög att det tränger igenom ballastlagret, vilket skulle medföra bärighets problem även för ballasten.

Abstract

As traffic loads along Malmbanan have increased over the years, and today LKAB wishes to further increase the tonnage of the ore cars. This has created problems in the rail superstructure and that this poses challenges to further increase traffic loads. In order to find solutions for a more sustainable railroad superstructure, which can handle these high traffic loads, which also creates high dynamic loads due to the length of the trains. An understanding of what happens in the underlying soil materials when exposed to dynamic loads is needed. Thus, the frequency analysis of accelerometer measurements from accelerometers is a possible method for analysing the impact of dynamic loads on underlying soil materials. Which provides knowledge of which soil materials are exposed to resonance because of the vibration of the trains and what possible problems this may cause.

For the analysis, two different sections along railway section 118 have been selected. Namely, section Tolikberget km 1222-1223 where Trafikverket has stated that there are problems in the railroad superstructure. As well as a reference section, where it should be good opportunities to verify that the method provides a reliable result. This section is Polcirkeln-Koskivaara km 1250+500-1251+600, which is dominated by a swamp area where the subsoil consists of large depths of peat, which is an advantage as it consists only of one type of soil material.

In addition, measurements have been analysed from stationary accelerometers at Notviken, which are mounted on a sleeper and a rail. Consequently, a comparison has been made between results from stationary measurements and measurements obtained from trains passing Tolikberget and Polcirkeln-Koskivaara. Which shows that it is possible to perform measurements in both ways to get desired information about the behaviour of the soil and other components during dynamic loading.

From the analysis of the selected sections at Tolikberget and Polcirkeln-Koskivaara, it is clear that the results correlate well with the expected values from the analytical calculations. Which confirms that the method can be seen as reliable as well as useful for further analysis.

The most critical consequence that can arise due to resonance of the subsoil on the sections at Tolikberget and Polcirkeln-Koskivaara, is liquefaction. Which through analysis could be confirmed. This would cause the subsoil to lose its bearing capacity which would lead to settlements. Also, there is a risk that the water pressure in the subsoil becomes so high that it penetrates the ballast layer, which would as well cause bearing capacity problems for the ballast.

Contents

1 Introduction

The effect of dynamics in the interactions between trains, rails, sleepers, ballast and subsoil can be analysed by frequency analysis. To be able to obtain frequency data from trains field measurements must be performed. At a moving train a suitable unit to measure is the acceleration of the bearings. Results that are obtained from these measurements are signals of accelerations in a time domain, which then must be converted into a frequency range before analysis. The measurement data of interest is the vertical acceleration, since this will give the needed information for evaluation of ground response. In the frequency range, the obtained signals are then divided in to different sections, since different response is connected to specific frequency range. (Angerhn, 2015)

The use of these measurements are mainly for monitoring the railway track condition, so that the condition of superstructures and rails are maintained with as little maintenance work as possible. (Angerhn, 2015) This is due to a challenge by having more infrastructural problems than there are funds available to maintain the railway network. (Gripner, 2012)

In Sweden, they have three different kind of measuring trains and these measure four specific parameters (Gripner, 2012):

- Rail profile, which measures equivalent conicity, height and side. These are measured every 3m along the rail.
- Track location data, which measures cant, gauge, height and- side position, shear, Q-value etc. These are measured every 25cm along the rail.
- Rippels and waves (corrugation), these are measured every 25cm, but are only presented every 10m.
- Ballast profile
- Overhead lines, which can be measured dynamically or statically. This is measured either every 2cm or 10cm along the rail.

By using a specific software in these measure trains so called “Optram”, there is a possibility to view multiple measurements simultaneously and combine different measurement parameters. In addition, analysis of the measurement data can be performed. Where one can analyse measurement data historically against other dependencies, as speed, against facility parts, for performing predictions based on historical data and as a control against limits.

Correlations between different parameters can as well be analysed by using Optram. One example can be “Does the quality number Q for the track location decrease faster in curves than in the straight lines?” (Gripner, 2012)

Ripples are detected by these measurements, since the accelerations are greater in the curves compared to straight lines along a railway, as well as the accelerations are larger at the inner rail in the curves. The development of ripples are therefore only associated with the inner rails in curves.

In addition, corrugations, rail cracks and track irregularities on the rails can be detected by analysing the results of vertical accelerations that are measured by the axel bearing and car body measurements.

From the monitoring of railway condition by these measurements, the changes in substructures or sleepers can be detected, in other words the vertical displacements. (Angerhn, 2015)

1.1 Aim and objective

The aim of this master thesis is to perform frequency analysis on obtained acceleration data from Trafikverket for two different sections along railway section 118, as well as on an additional data set from two stationary devices which are mounted on a sleeper and a rail. The objective is to determine how the soil layers are affected by the vibrations due to dynamic loading by trains, and thus consequences on the superstructure can be assesed.

1.2 Delimitations

The study is mainly limited to look into two different section along railway section 118, where one section works as a reference section. The locations of sections are chosen in cooperation with Trafikverket, since it is an advantage to analyse sections where the impact of dynamic loading is distinguishable, as well as they have an interest from Trafikverkets side to obtain knowledge of specific sections affected by dynamic loading. Therefore, section Tolikberget and Polcirkeln-Koskivaara is chosen for analysis.

But in addition, analyses will be performed at accelerometer measurements from stationary devices at Notviken, which are mounted on a sleeper and a rail. For each section along railway section 118, two analyses will be performed, one where the measurement is performed at the end of May and the other at the beginning of October. Because there is interest in seeing how the result differ between the period in May when the thawing is affecting the soil and the period in October when the soil has started to go in the freezing period.

The choice of code for Fast Fourier Transformation of acceleration data in the time domain is limited to a Matlab code, since it is a valid and available code.

The study is as well limited into literature review, gathering of theory, creating Matlab code, data treatment and frequency analysis.

1.3 Method

As an appropriate way to start a thesis, a project plan is first performed. This is done in cooperation with the supervisor, so that the content is adequate. Together with Trafikverket and the supervisor, relevant railway sections for the analysis are chosen. The geotechnical information/data and the accelerometer measurements for the chosen sections will be obtained through Trafikverket. For each section along railway section 118, the soil conditions will be determined and an assessment will be performed of what the expectations are from the frequency analysis. For the section at Tolikberget, length sections from Trafikverkets database will provide information about the soil conditions. For section Polcirkeln-Koskivaara, soil conditions will be obtained from the database. But there are no length sections available, so that the exact variation of the peat layers depth can be determined along the section. However, the available data provides maximum and minimum depth of the peat layer.

The theory is first used for the assessment of the expected results, where the assessment will contain calculations based on the theory and Technical requirements from Trafikverket.

Where the additional measurements are performed by the stationary devices at Notviken, no information of soil conditions are available. Therefore, the analysis part is focusing on looking into other possible parts which can be seen to show resonance.

For the frequency analysis of data, a Matlab code containing Fast Fourier Transformation and noise reduction will be performed. This code will be obtained from MathWorks and be verified by a person from the mathematical department at Luleå Technical University. With the results, where the accelerations are in the frequency band, due to the code, several analyses will be performed, to see if there are any correlations with the expected values and also if there are other parts that are excited into resonance.

2 Theory

Dynamic response analysis for soils is based on a single-degree-of-freedom model, which implies that the soil is modelled to consist of a spring, dashpot and a mass, so-called Voigt model (Figure 1). (Towhata, 2008) pp.89.

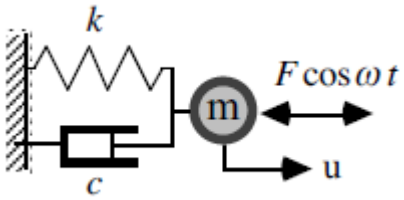

Figure 1. Voigt model. (Towhata, 2008)

When considering the elementary single-degree-of-freedom model for soils the dashpot is not considered (Figure 2). By this the resonance of soil is easier to describe due to amplification of the motion.

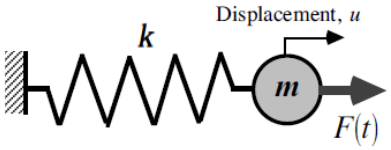

Figure 2.Elementary single-degree-of-freedom model. (Towhata, 2008)

As seen in Figure 2 the mass m is attached to a linear elastic spring k and by applying of a oscillatory force F(t) a displacement u will be achieved. If the oscillatory force is a sinusoidal function of time the mass will oscillate by a sinusoidal function which has a period T equal to $2\pi/\omega$. Where ω is the circular frequency which is derived from the relation to the frequency f that is the number of cycles per second and is equal to 1/T [$^1/_s = Hz$]. Therefore, the circular frequency ω is equal to $2\pi f$. If the shaking frequency ω becomes equal to the circular frequency which can be expressed for a spring-mass system also by, $\omega = \sqrt{^k/_m}$, an infinite amplification of the motion will occur or in other words the spring-mass system will be set into resonance (Figure 3).

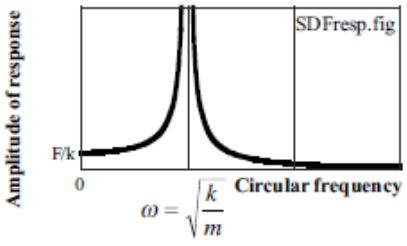

Figure 3. Amplification curve of a single-degree-of-freedom model. (Towhata, 2008)

Since resonance is a possible phenomenon that can occur in single-degree-of-freedom model or moreover in a soil it is important to prevent such events, because it might lead to rearrangements of the soil particles, which could cause significant settlements. (Towhata, 2008) pp.21.

The frequency based measurements have one challenge when it comes to the analysing part, which is that all components have different frequencies. The components have a eigenfrequency that must be known, but there are components frequencies that are also dependent of the speed. Therefore, by having a knowledge of different components frequencies, it makes it possible to assess what the source of a certain signal amplification is. (Angerhn, 2015)

A flexible railway track system is composed of different sublayers and components. According to (Profillidis, 2007) pp.33, the flexible railway consists of rails, sleepers, ballast, subballast, formation layer and base, where the two latter layers are related to the subgrade (see Figure 4).

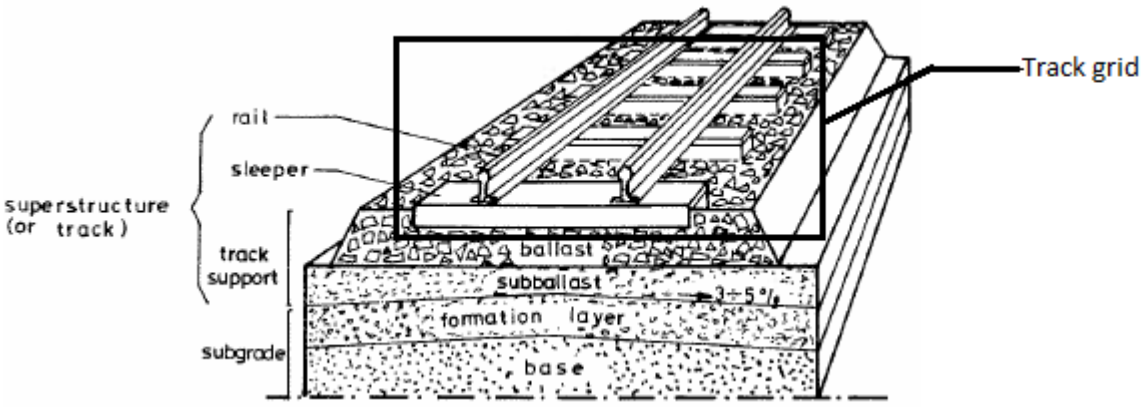

Figure 4. Flexible railway system. (Profillidis, 2007)

2.1 Frequencies with speed dependence

Components that has a dependency of the measuring trains speed are sleepers distance, track bumps and ripples. Sleeper base frequencies that occur due to sleeper distance and varies with the speed of the train can be obtained by a specific formula, where the trains speed and the sleeper distance must be known. As the rails are not continuous there are always gaps between rail segments, so called track bumps, and the frequencies due to these track bumps are also speed dependent. The formula for the sleeper base frequencies and track bumps is the same, but with a difference. For calculation of sleeper base frequency one must know the speed of the train and the sleeper distance. But for the frequency calculation due to track bumps one need to know the speed and the distance between the bogies. The equation of these frequencies is as follows:

$$f = \frac{1v}{3.6l} \left[{}^{1}/_{S} = Hz\right] \quad (1)$$

Where:

v, is the speed of the train [m/s]

l, is the distance between sleepers or the bogies [m]

Ripples is small irregularities at the rail surface, the frequencies caused by these ripples are dependent of the trains speed but also of the ripples wavelength. Ripples can occur in five different forms, which are Heavy Haul, Light Rail, Boosted Sleeper-Ripples, Roaring Rail, and Rutting-Ripples.

Heavy Haul Ripples have a frequency about 30 Hz and occurs at low constant speeds (30 km/h) with trains that have high loads (up to 40 t). If the trains are of lighter version (47 kg/m – 54 kg/m) along the railway, Light Rail Ripples occurs, and these cause frequencies between 30-50Hz. In the case of that the railway has a sharp curve (radius <400m) and sleepers which are founded at very soft sublayers and gravel-free track, Booted Sleeper Ripples occurs. The frequency range for Booted Sleeper Ripples is between 250 – 350 Hz. For high speed railways, Roaring Rail Ripples occurs and these has a frequency of 750 Hz. Ripples which are very common are so called Rutting Ripples, and the frequency range for these are 250 – 400 Hz. (Angerhn, 2015)

2.2 Eigenfrequencies of different components

All components have an eigenfrequency, which means that when the component is excited at its eigenfrequency it will start to vibrate. Therefore, it is important to have knowledge of components eigenfrequencies, so this phenomena could be avoided. In the case that the component does not have any damping, and is excited at its eigenfrequency, the component will go into resonance as well as the amplitudes will be infinite. Consequently, such an incident should be avoided. (Angerhn, 2015)

2.2.1 Eigenfrequency of sleepers

Sleepers are considered as undamped and this implies that the equation of eigenfrequency for sleepers is as follows:

$$f = \frac{1}{2\pi}\sqrt{\frac{EI}{mL^4}}\ [1/s = Hz] \qquad (2)$$

Where:

E: Young´s Modulus [N/mm^2]

m: Mass [kg/m]

L: Sleeper length [mm]

In railway constructions, there is used either wooden or concrete sleepers, but by calculations it is found that the eigenfrequencies does not differ much between these two types of sleepers. Therefore, an expected eigenfrequency for railway sleepers is 4 Hz. (Angerhn, 2015)

2.2.2 Eigenfrequency of the track grid

For the track grid, it is found that the eigenfrequency is between 60 and 90 Hz. (Angerhn, 2015)

2.2.3 Eigenfrequency of the superstructure

The eigenfrequency of a superstructure varies depending of the composition. The variation can be between 44 and 49 Hz, if the sleepers are made of concrete or wood with the same rail type. If the superstructure is made of a fixed road the eigenfrequency will be 78 Hz. (Angerhn, 2015)

2.2.4 Eigenfrequency of the train

Vibrations of a train are determined by whether they have suspension or not. For passenger trains an eigenfrequency between 1 and 2 Hz can be expected if the train has double suspension system. If the bogies do not have any suspension the expected eigenfrequency is between 5 and 10 Hz. (Angerhn, 2015)

2.2.5 Pinned-Pinned frequency

Since the wheels of the train will pass in between sleepers, a deflection of the rail will occur. Therefore, a bending wave arises that is the length of the deflection caused by the wheel load. If the bending wave length is equal to the double sleeper distance, a resonance of the vibration occurs, and the resonance frequency is about 1000 Hz. This Pinned-Pinned frequency is possible to calculate by the following equation: (Angerhn, 2015)

$$f = \frac{\omega}{2\pi} = \frac{1}{2\pi}\pi^2\sqrt{\frac{EI}{mL^4}}\left[{}^{1}/_{S} = Hz\right] \quad (3)$$

Where:

EI: Flexibility [MNm^2]

m: Mass [kg/m]

L: Sleeper distance [m]

2.2.6 Eigenfrequency of subsoil

For estimation of eigenfrequencies of subsoils a horizontal layered ground is considered, and the frequency is dependent of two factors in the soil, the shear wave velocity and thickness of the subsoil. The subsoils eigenfrequency is calculated as follows:

$$f_0 = \frac{v_s}{4H} = \frac{\sqrt{{}^{G}/_{\rho}}}{4H}\left[{}^{1}/_{S} = Hz\right] \quad (4.1)$$

Where:

$$\rho = \frac{1}{H}\sum_{i=1}^{n} \mathrm{Gi} * \mathrm{Hi}\left[{}^{kg}/_{m^3}\right] \quad (4.2)$$

$$G = \frac{1}{H}\sum_{i=1}^{n} \rho i * \mathrm{Hi}\ [^{kN}/_{m^2}] \qquad (4.3)$$

H: Total layer thickness of soft layers [m]

H_i: Layer thickness of the i-th layer [m]

G_i: Shear modulus of i-th layer [kN/m^2]

ρ_i: Density of the i-th layer [kg/m^3]

An empirical method can be used as well for the estimation of subsoil eigenfrequencies with varying depths. This is performed by using a chart (Figure 5). But the frequency values in this chart are very high, since the frequencies depend on different factors, like composition of the soil, moisture content and storage density. (Angerhn, 2015)

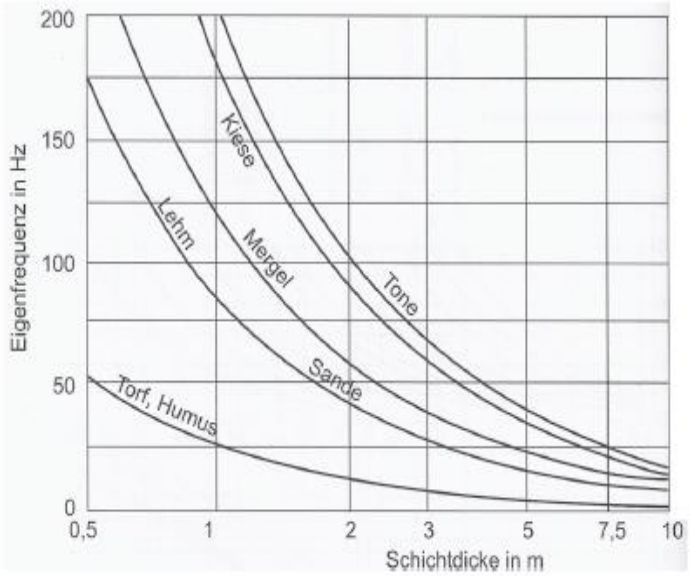

Figure 5. Eigenfrequency for subsoils with varying depth. (Lichtberger, 2005)

2.3 Shear wave velocities of gravel

As seen in the calculation of subsoil eigenfrequency, one important factor is shear wave velocity. If the stiffness of the soil decreases, then the shear wave velocity will decrease. (Angerhn, 2015)

According to (Richart & Woods, 1970) pp.153-155, the confining pressure and void ratio in sand material has a significant effect on the shear wave velocity. Furthermore, the shear wave velocity will decrease with increasing void ratio, as well as it will decrease when the confining pressure decreases. Consequently, the shear modulus will also decrease with increasing void

ratio and decreasing confining pressure, because the shear modulus is related to the shear wave velocity as follows:

$$G = \rho v_s^2 \ [\text{kN/m}^2] \quad (5)$$

Where:

G: Shear modulus [kN/m^2]

ρ: mass density [kg/m^3]

v_s: Shear wave velocity [m/s]

Studies of the influence by the degree of saturation in cohesionless soils on shear wave velocity, has according to (Richart & Woods, 1970) pp.156, shown that there is only a minor effect. They state that the small differences between the shear wave velocities for saturated and dry cohesionless soils, are due to the unit weight of water. Therefore, the unit weight and the average effective confining pressure of the soil is sufficient to consider, when evaluation of G and v_s must be performed.

2.4 Frequency analysis with bandwidths

Signals are analysed by using bandwidths, which can be octave bands or narrow bands. The function of bandwidths is that they work as filters, and this implies that in a certain frequency range only a few frequencies will be caught. The difference between octave band and narrow band is that octave band is a wider band than narrow band. Which means that octave bands can have a range between 16 – 16000 Hz with intermediate frequencies, and narrow bands might have a frequency range between 0 – 100 Hz. For octaves, a so called third octave band (Figure 6) can be used where frequency ranges are divided into smaller intervals, which consist of an upper and lower limit as well as a medium frequency. This suit well if constant amplitudes of the frequencies occur within the individual bands. But when there are frequencies which dominate others, narrow bands (Figure 7) are to prefer before third octave bands. (Angerhn, 2015)

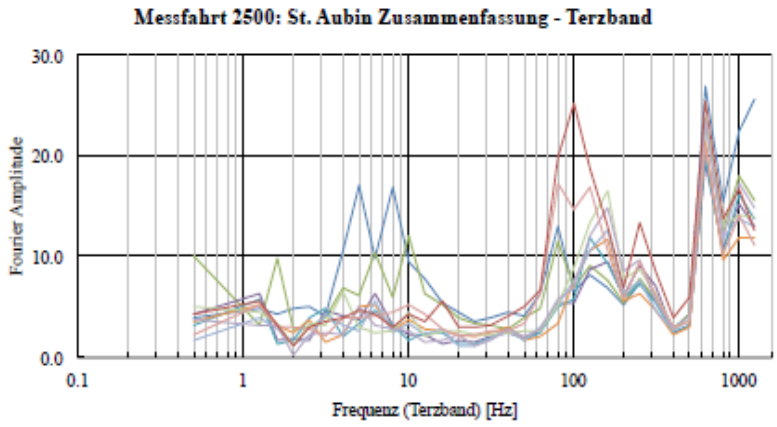

Figure 6. Third octave band, Measurement position tunnel St.Aubin, km 55.600-57.600 . (Angerhn, 2015)

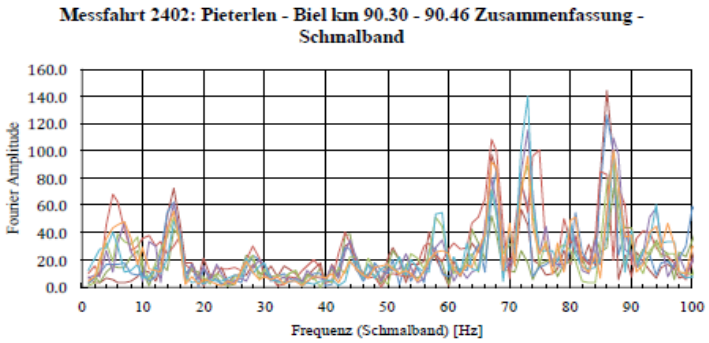

Figure 7. Narrow band, Measurement position Cornaux-Biel-Oensingen-Olten-Othmarsingen, km 83.800-104.500-27.500. (Angerhn, 2015)

2.5 Soil properties

For soils in the railway embankment and subgrade it is important to consider the dynamic loading and the consequences of it for the soil properties. What is already known, is that the shear modulus and shear wave velocities affect the eigenfrequency of the soil. Therefore, a softer material will reduce the shear modulus and shear wave velocities respectively, which leads to lower eigenfrequencies. Soft soils as clay and silt have lower shear modulus and by that lower eigen frequencies. On the contrary coarse grained soils as gravel and sand have higher shear modulus, they have also higher eigenfrequencies. But for coarse grained soils a deterioration of the material will occur under dynamic loading, which leads to formation of fine grained material in between the larger particles (Figure 8). Which causes a degradation of the shear strength, shear modulus as well as the bearing capacity and eigenfrequency.

Figure 8. Formation of fine material in between larger particles. (Angerhn, 2015)

As the ballast bed in the origin stage has grains which are of square and angular shape, it makes it more rigid. But due to dynamic loading, which causes deterioration of these square and angular shaped grains, that makes them rounder. The dilatancy angle decreases, which will lead to a contraction (settlement) of the ballast bed. Something that can be done as a counteract against the settlements is to use heavier rail profiles, longer sleepers or concrete sleepers.

Issues which can cause dynamic loads along railways are flat points formed on the wheels or poor design of rail welds.

As mentioned the ballast bed is of square and angular shape when it is new, the so called crushed gravel, and after deterioration it becomes rounder, the so called round-grained gravel. A relationship exists between shear modulus, pore space and major mean effective stress, for

both types of ballast gravel. Which is then interpreted for eigenfrequency calculations as mentioned earlier. The equations for calculating the shear modulus for crushed gravel and round-grained gravel are as follows:

Crushed gravel:

$$G_{max} = \frac{3260(2.97-e)^2}{1+e}(\sigma_m^{'})^{0.5}\ [kN/m^2] \quad (6.1)$$

Round-Grained gravel:

$$G_{max} = \frac{7000(2.17-e)^2}{1+e}(\sigma_m^{'})^{0.5}\ [kN/m^2] \quad (6.2)$$

Performed analysis of crushed gravel and round-grained gravel has shown a difference in the eigenfrequency of 5-6 Hz between these gravel types. But a larger difference in the eigenfrequency is instead observed individually for both gravel types, by changing the layer thickness. Independently of gravel type the eigenfrequency decrease by 20 Hz with a 10cm increase in layer thickness. However, when the crushed gravel deteriorates into round-grained gravel it will bring the same rate of change in eigenfrequency as changing the layer thickness by 2-3cm.

The subgrade is affected by dynamic loading as well, depending of the type of soil it consists of, the settlements and deformations will vary. Therefore, soils in the subgrade must be considered as well, to prevent unwanted damage on the railway embankment. (Angerhn, 2015)

For granular materials, there has been performed studies for the effects of number of load applications on permanent strain. According to (Lekarp et al.) the growth of permanent deformations are due to small increments of accumulated strains by repeated loading. They also state that for low stresses a stabilization of the growth of permanent deformation can be achieved, but higher stresses will cause a gradual deterioration and continues increase of permanent strain.

Axial loading tests on confined samples of cohesionless soils has been performed by Whitman and co-workers, the result from the test provides that with increasing number of load cycles the permanent vertical strain increases. This means as well that the volume will decrease with increasing number of load cycles due to the confinement in the test, which does not allow any lateral deformations. (Richart & Woods, 1970) pp.180-182.

According to (Richart & Woods, 1970) pp.182-184, vibrational and impact loads that consist of peak accelerations, which are products of the amplitude and the frequency squared, has an influence on the volume change in cohesionless soils. The size of volume change is also dependent on the soil mass initial void ratio, confining pressure, characteristics of the soil and the dynamic loads intensity. However, the test results regarding the volume change due to vibration and impact loads, were peak acceleration is kept constant by changing either the frequency or the amplitude. Shows that the frequency has little effect on the deformation behaviour of unsaturated granular material, instead the most significant impact is due to the amplitude. From the tests, it was obtained that the soil decreased in volume with increasing peak acceleration, these results are presented either by plotting peak acceleration vs. unit weight or peak acceleration vs. void ratio. With increasing peak acceleration, the unit weight increases up to a certain level were either a loosening of soil occurs and the unit weight decreases or that the soil volume just continues to decrease. In the other plot the void ratio decreases with increasing peak acceleration, which means that the volume decreases.

Liquefaction is a phenomenon that must be considered for cohesoinless soils. If a saturated soil loses its shear strength, then it will become into a liquefied state as a fluid. From the equation of shear strength for a cohesionless soil this becomes clear, which is as follows:

$\tau = (\sigma - u)tan\varphi'$ [kPa] (7)

Where:

τ: Shear strength [kPa]

σ: Total stress [kPa]

u: Pore pressure [kPa]

φ': Effective angle of internal friction [º]

If the pore pressure increases, the shear strength will be decreased, and in the worst case it will reduce the shear strength to zero when it becomes equal to the total stress, in this state the cohesionless soil will behave like a fluid. The consequences of liquefaction are that the soil loses its bearing capacity and structures which are founded on the soil will settle.

Dynamic and impact loads are sources that can cause liquefaction in saturated cohesionless soils. What happens in a soil skeleton when it is exposed to dynamic loading, is that it will be disturbed and rearranged into a denser state by compaction of the particles. As the particles are moving during a rearrangement they will temporarily be in part supported by the pore water, which in turn causes a pore pressure increase by transmission of the loads to the pore water. Therefore, the ability of compaction of the soil is a factor that determines the liquefaction potential. From studies, conclusions of the determining factors are obtained, regarding the ability of compaction of saturated sand. The factors that are significant to consider, are the intensity of the dynamic load, initial void ratio and the confining pressure. (Richart & Woods, 1970) pp.172-174.

2.6 Acceleration measurement

To obtain suitable measurement data for frequency analysis a convenient measurement device to be used is an accelerometer. By mounting these accelerometers on the structures with vibrations the measurement itself can be done. Since the vibrations will be transmitted into the accelerometer which in turn will start to accelerate. The quantity of accelerations can either be in m/s^2 or g, and these are measured in the time domain. To obtain accurate results from a measurement it is important to consider the installation of an accelerometer as well as the choice of transducer. Two types of accelerometers are the Piezoelectric and Micro Electro-Mechanical systems (MEMS), where the former is analogue and the latter is digital. To cover the basic principles of how an accelerometer works, a description of the piezoelectric model will be done.

There are three different designs of Piezoelectric accelerometers, either it is of a planar/delta shear design or of a compression design.

The basis for both shear design accelerometers (Figure 9) is that the piezoelectric elements and seismic masses are attached to a centre post which are held in place by high tensile clamping rings. The assembly of centre post, piezoelectric elements and seismic masses are founded on a base and they are as well encapsulated by a housing.

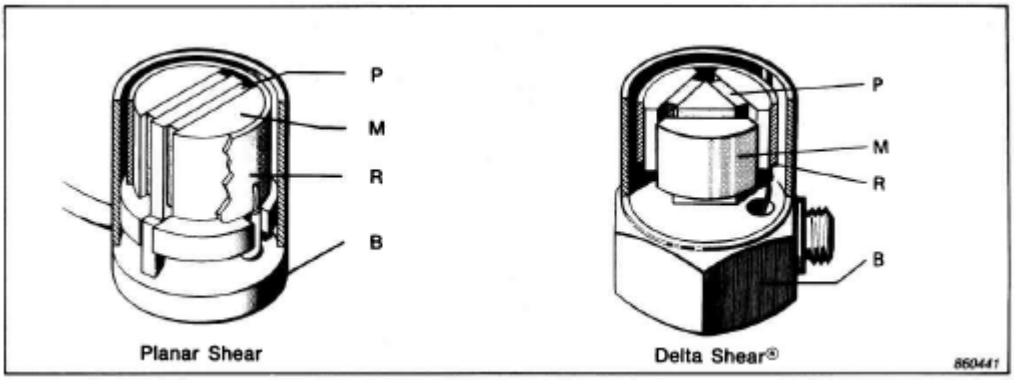

Figure 9. Planar and Delta Shear accelerometers. (Serridge & Licht, 1987)

A compressional designed accelerometer (Figure 10) has as well the piezoelectric elements and seismic masses attached to a centre post, but in this case the centre post is of cylindrical shape instead of rectangular or triangular one.

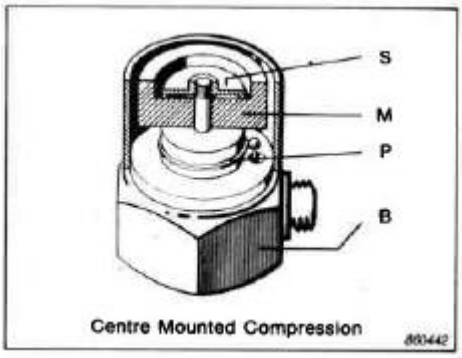

Figure 10. Compressional accelerometer. (Serridge & Licht, 1987)

From the vibrations an accelerometer is subjected to, a force is created, which acts on the piezoelectric elements and is defined as the product of the acceleration of the seismic masses and the mass of the accelerometer. By these forces the piezoelectric elements will produce a charge and is therefore proportional to the applied force. The charge is as well proportional to the acceleration of the seismic masses, since the masses are constant. Finally, the output from an accelerometer is proportional to the acceleration of the surface, where the accelerometer is mounted. Since the surface and the base of an accelerometer is in connection and the base acceleration has the same magnitude and phase as the seismic masses.

As mentioned the piezoelectric elements produce a charge when they are subjected to forces, because these elements are polarized ceramics. In (Figure 11) an illustration can be seen of three polarized piezoelectric elements. Wherein the upper is one in undeformed state, which has the polarized domains unaffected. The lower ones are affected by external forces due to the accelerations, which causing the domains to deform. By this, charges of opposite polarity will be formed on each side of the element and they will be collected by the contact. The element on the left underneath in the figure has a compressional force acting on it. To the right underneath in the figure the element is affected by a shear force. However, what these two cases have in common, is that the charges are developed along the surfaces where the forces act.

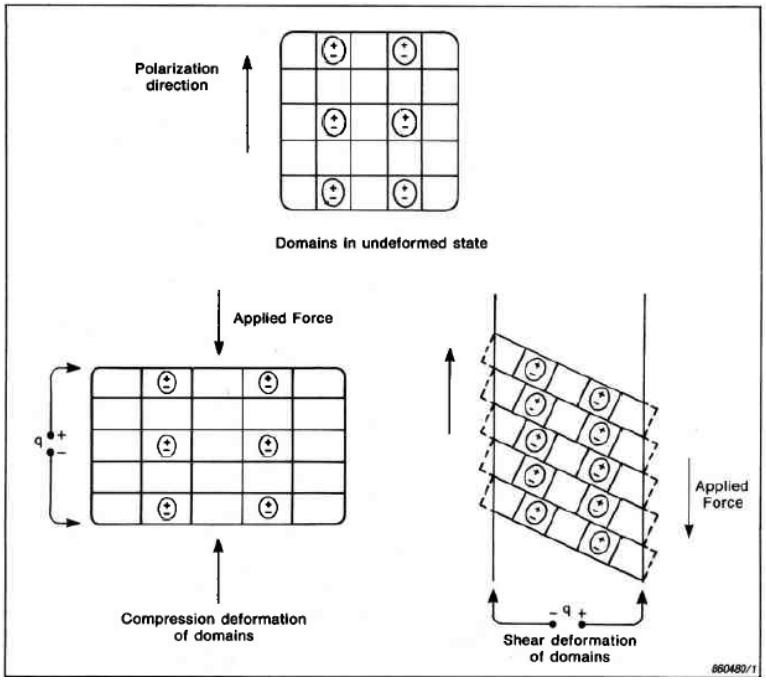

Figure 11. Polarization of piezoelectric elements. (Serridge & Licht, 1987)

Physically the piezoelectric accelerometers can be modelled by two unsupported masses which are connected with an ideal spring, where the systems damping is neglected. The model is illustrated in Figure 12 (Serridge and Licht), where:

m_s= total seismic mass [kg]

m_b= mass of the accelerometer base [kg]

x_s= displacement of the seismic mass [m]

x_b= displacement of the accelerometer base [m]

L= distance between the seismic mass and the base when the accelerometer is at rest in the inertial system [m]

F_e= harmonic excitation force [N]

F_0= amplitude of excitation force [N]

ω= excitation frequency (rad/s) = $2\pi f$

ω_n= natural resonance frequency of the accelerometer (rad/s)

ω_m= mounted resonance frequency of the accelerometer (rad/s)

k= equivalent stiffness of the piezoelectric elements [N/m]

F= k (x_s- x_b-L) spring force [N]

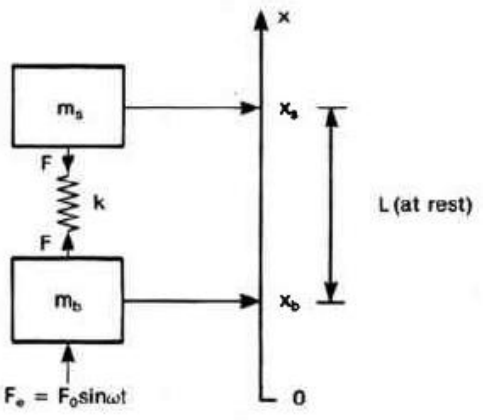

Figure 12. Physical model of piezoelectric accelerometer. (Serridge & Licht, 1987)

This model is based on the equation of motion and the first step is to begin from its free vibration position, where the accelerometer is hanging freely and has no external force impact. Due to assumptions, regarding displacements of the seismic mass relative to accelerometer base mass, the differential equation of motion can be solved. Which leads to a solution for the natural resonance frequency of the accelerometer, $\omega_n^2 = k(\frac{1}{m_s} + \frac{1}{m_b})$. This equation changes when the accelerometer is mounted with very good rigidity on a structure, if the structure is heavier than the accelerometer then m_b will be much larger than m_s. Therefore, a lowering of the accelerometers resonance frequency will occur. For the case where the structures weight is

assumed to be infinite, the resonance frequency of the accelerometer becomes, $\omega_m^2 = \frac{k}{m_s}$ and is called the mounted resonance frequency.

When a vibration of the accelerometer is affected by an external force, the equation of motion will lead to a relation together with assumptions of the displacements of the seismic masses and accelerometer masses. This relation consists of a ratio between displacements at low frequencies R_0 and high frequencies R, $\frac{R}{R_0} = \frac{-\frac{F_0}{m_b(\omega_n^2 - \omega^2)}}{-\frac{F_0}{m_b\omega_n^2}}$. However, low frequency displacements are related to frequencies much below the natural resonance frequency ($\omega \ll \omega_n$). Therefore, by rearrangement of the expression, one can obtain, $\frac{R}{R_0} = \frac{1}{1-(\frac{\omega}{\omega_n})^2}$.

From this equation it is possible to see, that when the forcing frequency becomes close to the natural frequency of the accelerometer, an increase of the displacement between the seismic mass and the base occur. Which also means that an increase is obtained on the forces acting on the piezoelectric elements and the electrical output from the accelerometer. This is as well illustrated in (Figure 13) which shows the frequency response curve of an accelerometer. (Serridge & Licht, 1987)

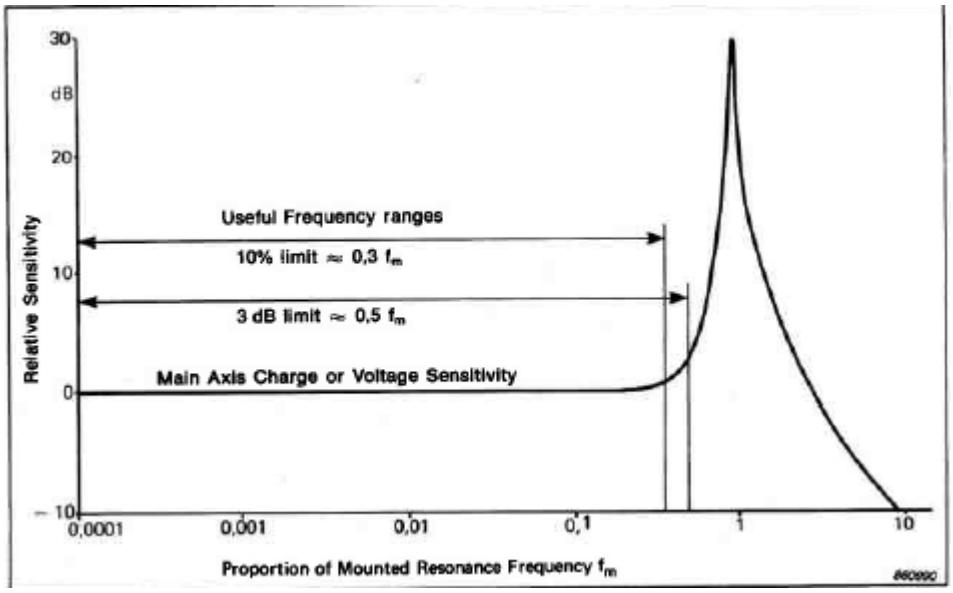

Figure 13. Frequency response curve of an accelerometer. (Serridge & Licht, 1987)

3 Data treatment

3.1 Fast Fourier Transformation

When the measurement data is recorded in the time domain, a transformation of the signal is needed, to obtain a representation of the signal in a frequency domain. The signal from the time domain is decomposed into a sum of cosines and sines of various frequencies by the Fourier transformation.

Fourier transformations can be performed by either a Discrete Fourier Transformation or by the Fast Fourier Transformation. The difference between these two methods is that the Discrete Fourier Transformation requires a longer computational time compared to the Fast Fourier Transformation. If the Discrete Fourier Transformation uses the trapezoidal rule on N data points, it does N multiplications and N additions i.e. N^2 computations. For N data points the Fast Fourier Transformation applies an algorithm of $N\log_2(N)$ operations. Let say that the number of data points are 1000, then the Discrete Fourier Transformation needs 1000000 computational operations and the Fast Fourier Transformation needs approximately 10000 operations. This implies that Fast Fourier Transformation reduces the computational time, which is an advantage in analysis. (Storey, 2017)

3.2 Application of Fast Fourier Transformation in Matlab

The measurement data that is measured in the time domain must be transformed into the frequency domain. For the transformation of data, the code Matlab is used, where the data first is imported and then by Fast Fourier Transformation the data is transformed into the frequency domain (MathWorks, 2017a). After the transformation, the data has much noise which makes it difficult to read the graphs. To reduce the noise and obtain a smoother curve in the frequency domain, a code named “pwelch” is used in Matlab. Which returns a clearer and smoother curve that is easier to read by splitting the signal into segments which are multiplied by Hamming windows (MathWorks, 2017b).

As a first step, data from El Centro earthquake 1940 was used for the spectral analysis, for a verification of that the Fast Fourier Transformation and pwelch code in Matlab work correctly. The data of El Centro earthquake was obtained from Vibrationdata.com (Vibrationdata, 2017), the data for this earthquake was given in the time domain, where the Peak Ground Acceleration was measured. By importing the data into excel, the data where sorted into two separate columns, as well as a graph of peak ground acceleration vs. time could be obtained (Figure 14). For spectral analysis in Matlab the column vectors from excel was used, by importing the data into Matlab. By taking Fast Fourier Transformation of the data the graph of spectral amplitude vs. frequency could be obtained (Figure 15). As it is seen, the graph contains much noise, which by using the pwelch code was reduced to a clearer and smoother curve (Figure 16). For verification of the accuracy of this spectral analysis, associate Prof. Niklas Grip from the Math Dept at LTU provided assistance. Thus, the reliability of the Matlab code was confirmed. Therefore, is the Matlab code (Appendix 2) used further in the work in this Master Thesis.

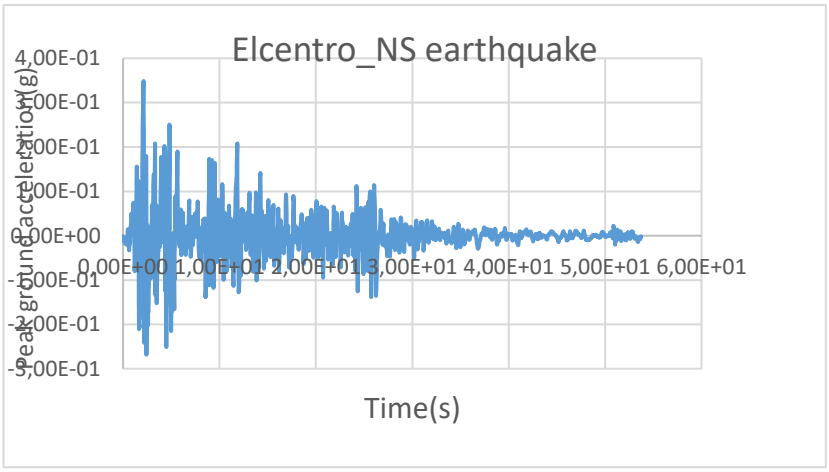

Figure 14. Peak ground acceleration vs. time, El Centro earthquake 1940. (Vibrationdata, 2017)

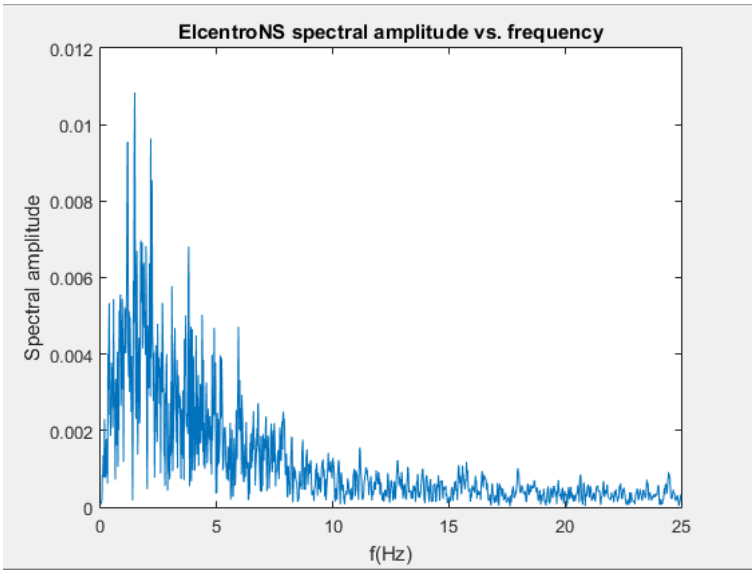

Figure 15. Spectral amplitude vs. frequency.

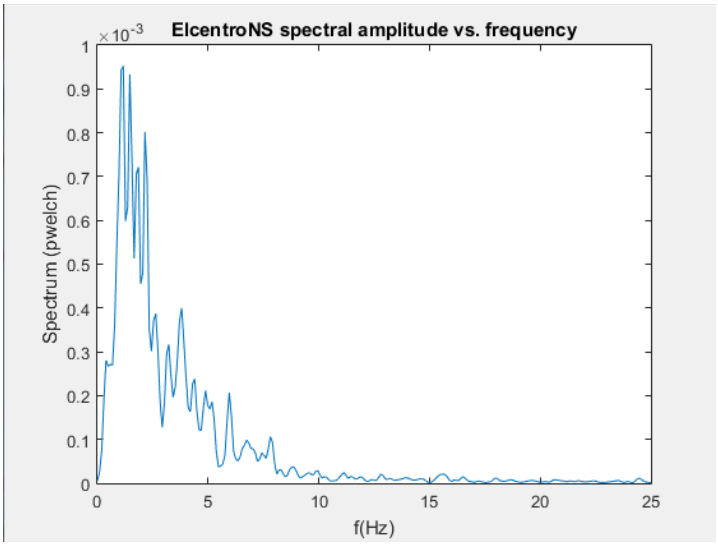

Figure 16. Spectral amplitude(pwelch) vs. frequency

4 Malmbanan

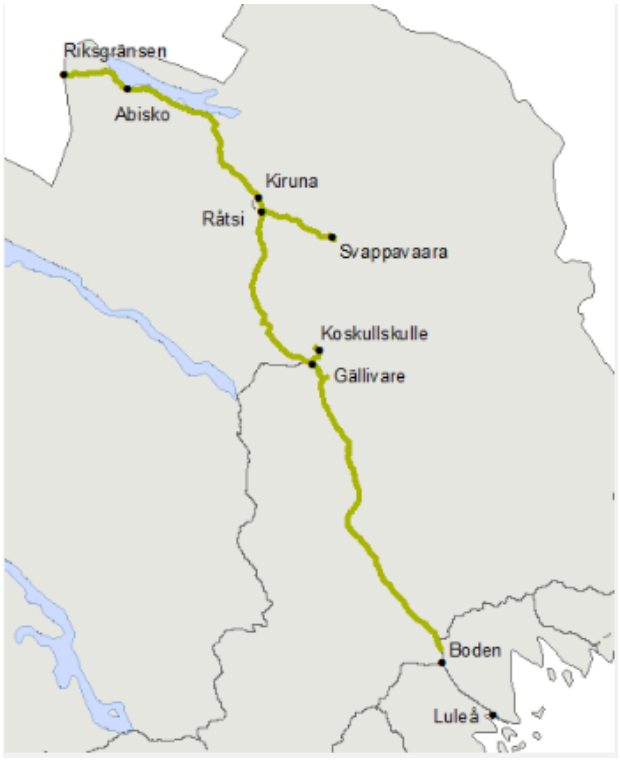

Figure 17. Malmbanan. (Trafikverket, 2017)

Malmbanan (Figure 17) is a railway system in the northern part of Sweden and is located between Boden and Riksgränsen. The length of this railway system is 500 km and have a variety of different trains running along the railway, as freight trains, passenger trains and ore trains. The amount freight tonnage along this railway system is 15 million net tonnage ore per year between Kiruna and Narvik, and 7 million net tonnage per year between Luleå and Kiruna. This railway system is an electrified single track with sidings. The special feature of this railway system is that it is the only one in Sweden that allows today 30 ton axel load and a total amount of 8600 heavy train passages. The length of each ore train is 750m including 68 wagons, which means that the sidings plays an important role for a good capacity of the traffic along Malmbanan. Daily ore train traffic between Kiruna and Narvik amounts to 22 and between Malmberget and Luleå up to 10 ore trains.

Currently Trafikverket and LKAB have an ongoing project, where the purpose is to investigate the possibility to increase the axle load on the ore trains from 30 tons up to 32.5 tons. This is performed by operate two trains per day between Vitåfors and Luleå with an axle load of 32.5 tons. If this improvement in increased axle load would be possible, then each ore train could transport additional 680-ton ore. (Trafikverket, 2017)

In this master thesis two railway sections will be analysed which lies along Malmbanan, the first one is Tolikberget and the second is Polcirkeln-Koskivaara. In the map below (Figure 18) the locations of these sections can be seen, descriptions of these are written in detail in the next chapters.

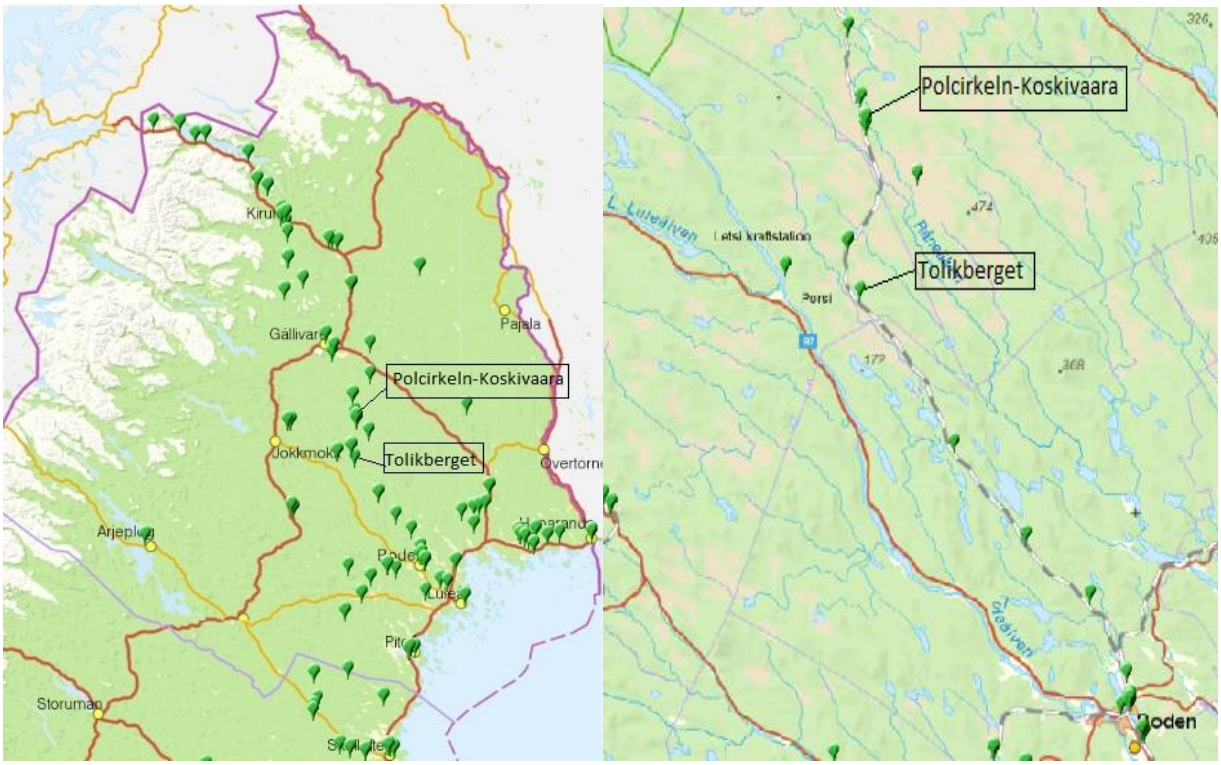

Figure 18. Location of Tolikberget and Polcirkeln-Koskivaara. (Trafikverket, Geoteknisk Databas, 2017)

4.1 Tolikberget km 1222-1223

Tolikberget is located along railway section 118, which is the part of Malmbanan located between Boden and Gällivare. This area consists of undulating forest terrain and when you go north, the terrain to the right of the railroad is open, since a power line follows along the railway. Along most of the stretch, there is also a gravel road following the railway at the right-hand side towards north. (Figure 19) (Trafikverket, Järnvägsfilm Bandel 118 , 2016)

Figure 19. View of Tolikberget. (Trafikverket, Järnvägsfilm Bandel 118 , 2016)

The superstructure along this section consist mainly of a ballast layer of 0.4 meters at the top. Underneath the ballast, a layer of gravelly silty sand from 1.0 to 2.1 meters can be found. Where the groundwater table is located directly below the ballast layer. Between km 1222+180 and km 1222+700 there is a layer of peat which starts at a depth of 2.0 meters below the rail bottom. A layer of coal ash is located between km 1223+050 and km 1223+250, which starts 1.0 meters beneath the rail bottom, and the material beneath the coal ash consists of gravelly silty sand which transforms into a layer of rocky gravelly silty sand. By the soundings, stop against rock or blocks at a maximum depth of 7.3 meters beneath the rail bottom has been obtained between km 1222+180 and km 1222+920. At a maximum depth of 3.8 meters below the rail bottom, a stop has been obtained against rock or blocks from the soundings between km 1222+920 and km 1223+380. (Noppa, 2003)

The groundwater table along this section is located directly below the ballast layer.

A general view over the soil stratigraphy for the railway embankment along this section can be seen in (Figure 20).

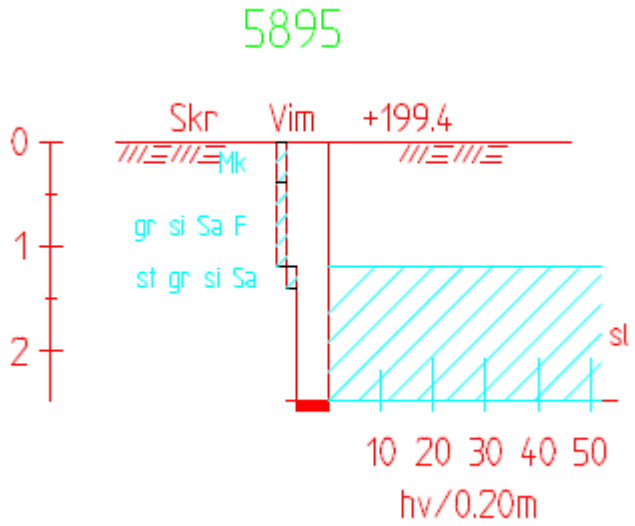

Figure 20. General soil stratigraphy for Tolikberget railway embankment km 1222+350. (Trafikverket, Geoteknisk Databas, 2017)

4.1.1 Expected eigenfrequency of subsoil and ballast

From this railway section one survey point is used to show how the subsoil is composed in general along Tolikberget km 1222-1223. Thus, for representation of the soil stratigraphy for the calculations of the eigenfrequency, survey point 5895 is chosen (Figure 20). The subsoil consists of 2 meter thick layer of gravely silty sand, which is covered by a 0.5 meter thick ballast layer on top.

According to the calculations of subsoil and ballast eigenfrequencies (Appendix4), the expected values for subsoil and ballast are 26.46 Hz and 119.80 Hz, respectively.

Tabell 1. Expected eigenfrequency for subsoil and ballast, Tolikberget km 1222+300-1222+400.

Expected eigenfrequency for subsoil and ballast, Tolikberget km 1222+300-1222+400. [Hz]	
Subsoil	26.46 Hz
Ballast	119.80 Hz

4.1.2 Result of frequency analysis km 1222+300-1222+400

The analysis along Tolikberget is performed for the part km 1222+300-1222+400, which covers the soil conditions for the investigation point shown in (Figure 20) that is used for the calculations of expected eigenfrequencies. The acceleration measurements are performed in late May 2016 and in the beginning of October 2016, to see if there are differences between the thawing period and the beginning of the freezing period. The data is as well obtained from both sides of the railway track, which means that measurements are performed for both left and right side. The average speed of the measurement train is considered as well, since the speed of the train can affect the results. Therefore, by calculations, the average speed is obtained for measurements in May and October when it passes km 1222+300-1222+400. In May, the measurement train had an average speed of 123.84 km/h and in October 117.97 km/h, which can be seen below by the calculations.

Km 1222+300-1222+400 May:

Time elapsed: 2.907 s

Distance: 100m

$$Speed = \frac{Distance(m)}{Time(s)} = \frac{100}{2.907} = 34.40\,{}^{m}/_{s} = 123.84\,{}^{km}/_{h}$$

Km 1222+300-1222+400 October:

Time elapsed: 3.052 s

Distance: 100m

$$Speed = \frac{Distance(m)}{Time(s)} = \frac{100}{3.052} = 32.77\,{}^{m}/_{s} = 117.97\,{}^{km}/_{h}$$

Results of the FFT on the signals from km 1222+300-1222+400 for the frequencies below 100 Hz, which covers the eigenfrequencies of the soil, are presented below.

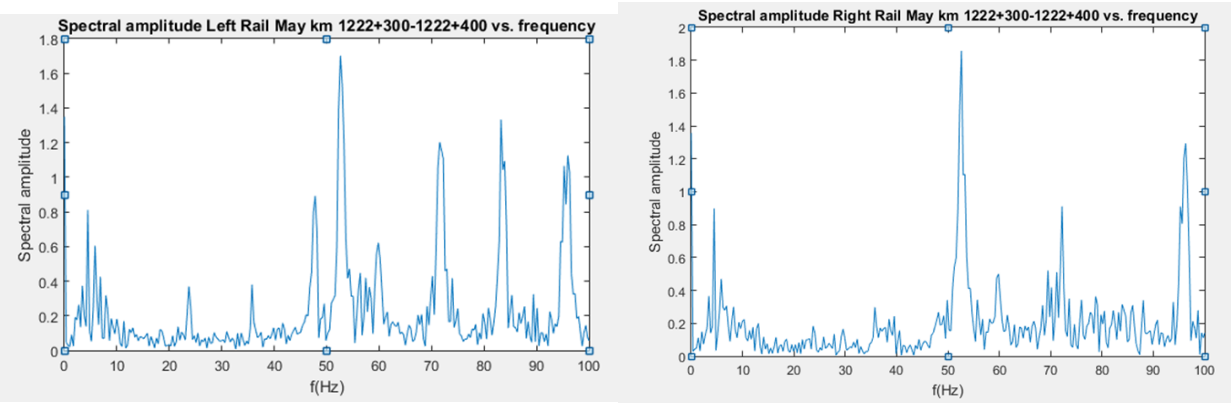

Figure 21. Results of frequency analysis between 0-100 Hz, Tolikberget km 1222+300-1222+400 May 2016.

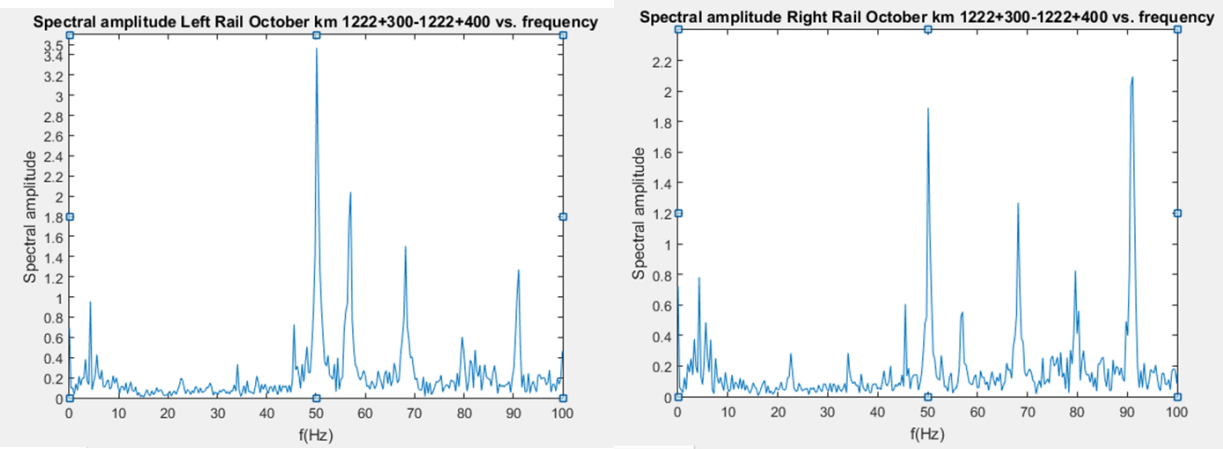

Figure 22. Results of frequency analysis between 0-100 Hz, Tolikberget km 1222+300-1222+400 October 2016.

Results of the FFT on the signals from km 1222+300-1222+400 for frequencies between 100 and 450 Hz, where other components eigenfrequencies emphasize more.

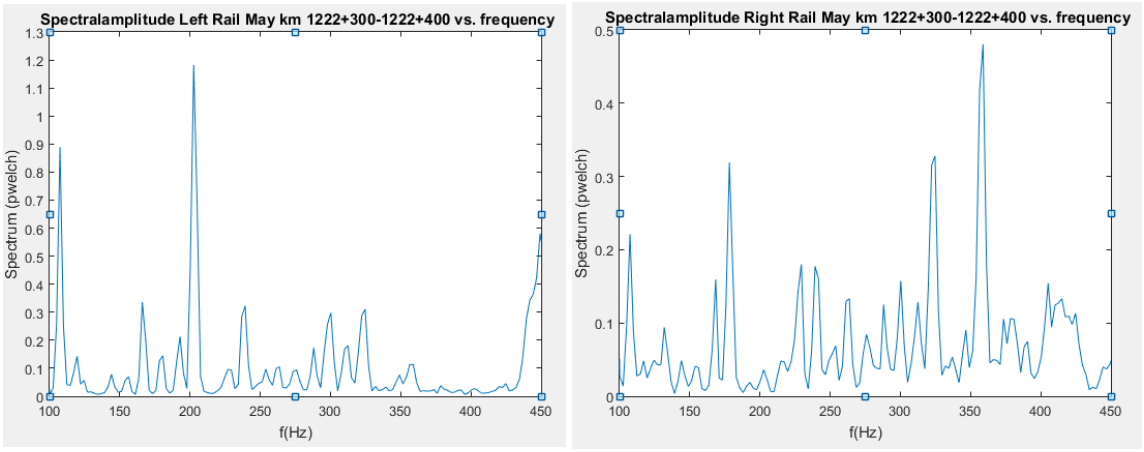

Figure 23. Results of frequency analysis between 100-450 Hz, Tolikberget km 1222+300-1222+400 May 2016.

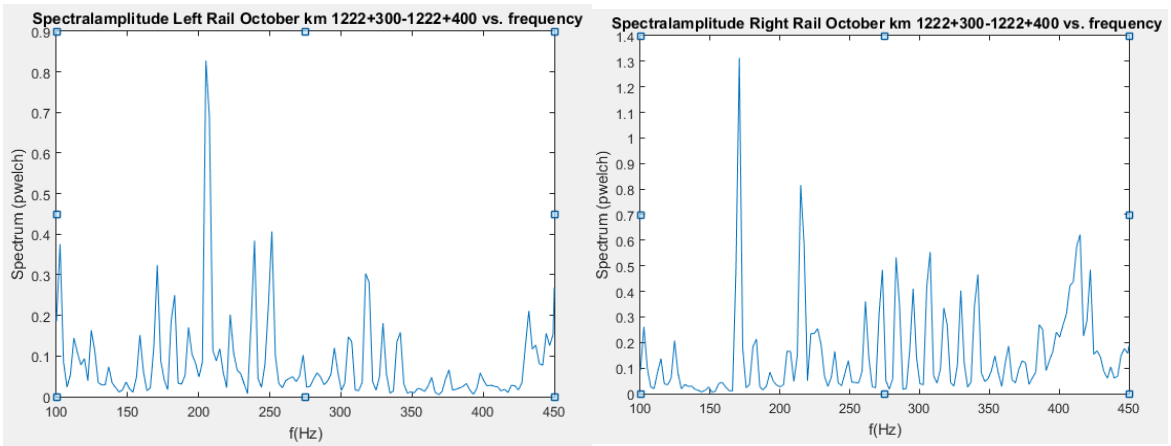

Figure 24. Results of frequency analysis between 100-450 Hz, Tolikberget km 1222+300-1222+400 October 2016.

Results of the FFT on the signals from km 1222+300-1222+400 for frequencies up to 2500 Hz, where other components eigenfrequencies emphasize more.

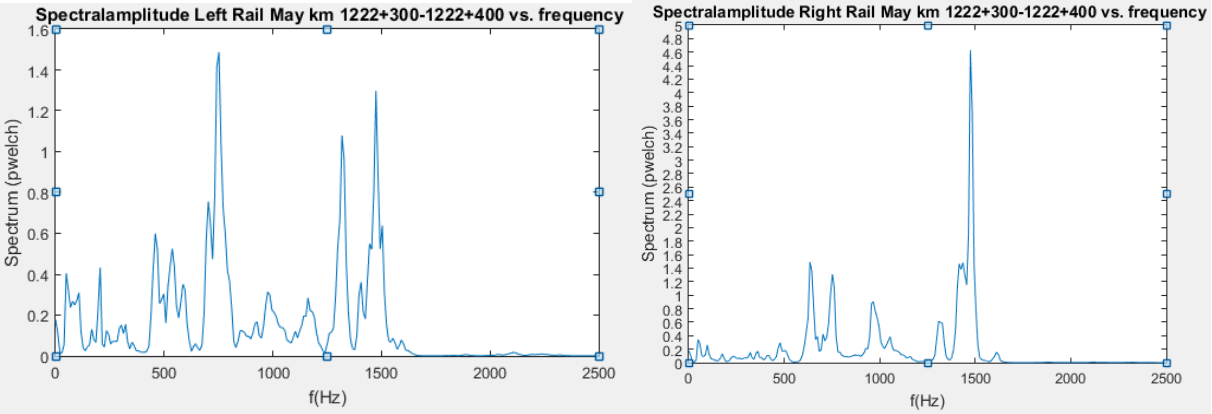

Figure 25. Results of frequency analysis between 0-2500 Hz, Tolikberget km 1222+300-1222+400 May 2016.

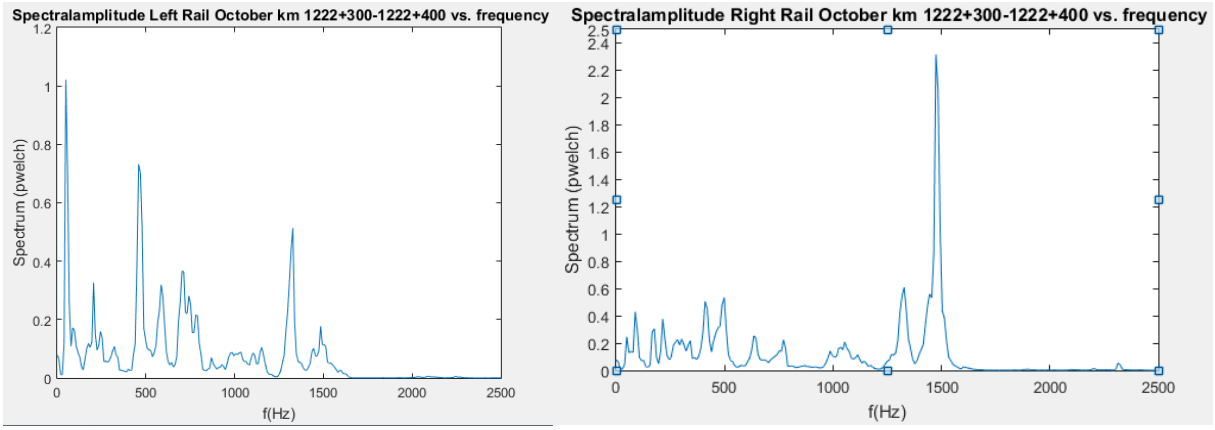

Figure 26. Results of frequency analysis between 0-2500 Hz, Tolikberget km 1222+300-1222+400 October 2016.

4.2 Polcirkeln-Koskivaara km 1250-1251

Polcirkeln-Koskivaara is a section which is located further north along Malmbanan, which consist as well for one part of undulating forest terrain with some areas of clear cuts. However, along this section a dominating part consists of a swap area (Figure 27), km 1250+980 to km 1251+400, where the railway embankment is quite low, from 0.5 meters to 1.5 meters. According to (Gustafsson, Engström, & Finnberg, 2016) the ground water table follows the surface of the swamp.

Figure 27. View of Polcirkeln-Koskivaara. (Trafikverket, Järnvägsfilm Bandel 118, 2012)

The swap area consists mainly of peat, and the geotechnical surveys performed by stick sounding and machine driven weight sounding shows the peat layers depth along the swamp. The depth of the peat layer varies from 0.7 meters up to 5.48 meters, between km 1250+800 to km 1251+520. (Trafikverket, Järnvägsfilm Bandel 118, 2012) (Gustafsson, Engström, & Finnberg, 2016)

The railway embankment along the swamp area is founded on a timber bed which lies directly on the peat. How the stratigraphy can look like along the swamp area is illustrated in (Figure 28), which is a picture of a geotechnical survey from this section. (Trafikverket, Geoteknisk Databas, 2017)

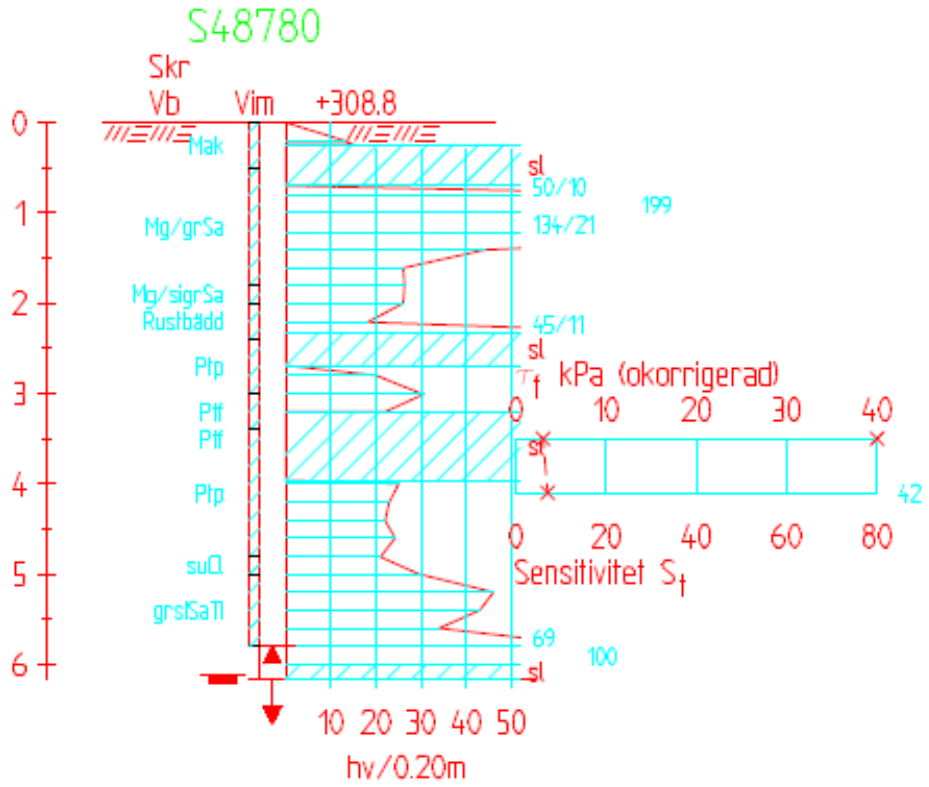

Figure 28. Stratigraphy of the soil along the swamp area at Polcirkeln-Koskivaara. (Trafikverket, Geoteknisk Databas, 2017)

4.2.1 Expected eigenfrequency of subsoil and ballast

Since this railway section is along a swamp area consisting mainly of peat underneath the embankment, survey point S48780 is chosen to represent the soil stratigraphy. According to Figure 28 the peat layer is about 2.5 meter thick covered by layers of ballast and made ground, which are 0.5 meter and 1.5 meters thick, respectively. But for the expected eigenfrequency calculations, there is as well considered how the eigenfrequency changes if the peat layers thickness is 0.7 meters or 5.48 meters.

What is seen from calculations (Appendix5), is that the eigenfrequency would be expected to be between 6.81 and 52.63 Hz when the water content is 863.1 percent, and between 8.74 to 67.56 Hz with a water content of 409.5 percent. A comparison of these values with the guideline values for peat in (Figure 5) shows that these obtained values are in the same range. Therefore, it is relevant to expect that the eigenfrequency of peat along Polcirkeln-Koskivaara should be between 6.81 and 67.56 Hz.

From the eigenfrequency calculations regarding the ballast layer (Appendix5), it appears that the expected eigenfrequency of ballast along Polcirkeln-Koskivaara should be between 44.5 and 101.3 Hz. The values of calculated eigenfrequencies are shown in table.2 and table.3.

Tabell 2. Expected eigenfrequencies for peat, Polcirkeln-Koskivaara km 1251+200-1251+300.

Expected eigenfrequencies of peat [Hz]				
Layer thickness of peat [m]	Water content 863.1%		Water content 409.5%	
	Density 1100 kg/m^3	Density 1300 kg/m^3	Density 1100 kg/m^3	Density 1300 kg/m^3
0.7	52.63 Hz	48.90 Hz	67.56 Hz	62.78 Hz
2.5	14.90 Hz	14.20 Hz	19.20 Hz	18.20 Hz
5.48	6.95 Hz	6.81 Hz	8.92 Hz	8.74 Hz

Tabell 3. Expected eigenfrequencies for ballast, Polcirkeln-Koskivaara km 1251+200-1251+300.

Expected eigenfrequencies for ballast [Hz]	
Thickness of ballast layer [m]	Frequency [Hz]
0.5	101.34 Hz
1.5	44.46 Hz

4.2.2 Result of frequency analysis km 1251+200-1251+300

Along Polcirkeln-Koskivaara the analysis is performed at a 100m part of the swamp, namely km 1251+200-1251+300. Since the depth of the peat layer along this section varies between 0.7m to 5.48m, a good average value is 2.5m, which is used in the calculations of expected eigenfrequencies according to survey point S48780 (Figure 28). For this section, measurements of the accelerations are performed in late May 2016 and in the beginning of October 2016. Since there is an interest for this section as well to see differences between the thawing period and the beginning of the freezing period. The measurements are obtained from both left and right side of the railway track. Since the speed of the train can affect the results, the speed of the measurement train is considered as well for this section. Therefore, when the measurement train passes km 1251+200-1251+300, the average speed is obtained by calculations, this is performed for measurements done in May and October. The average speed of the train in May and October is 30.65 km/h and 43.27 km/h, respectively. These calculations are shown below.

Km 1251+200-1251+300 May:

Time elapsed: 11.744 s

Distance: 100m

$$Speed = \frac{Distance(m)}{Time(s)} = \frac{100}{11.744} = 8.51\,{}^{m}/_{s} = 30.65\,{}^{km}/_{h}$$

Km 1251+200-1251+300 October:

Time elapsed: 8.319 s

Distance: 100m

$$Speed = \frac{Distance(m)}{Time(s)} = \frac{100}{8.319} = 12.02\,{}^{m}/_{s} = 43.27\,{}^{km}/_{h}$$

Results of the FFT on the signals from km 1251+200-1251+300 for the frequencies below 100 Hz, which covers the eigenfrequencies of the soil, are presented below.

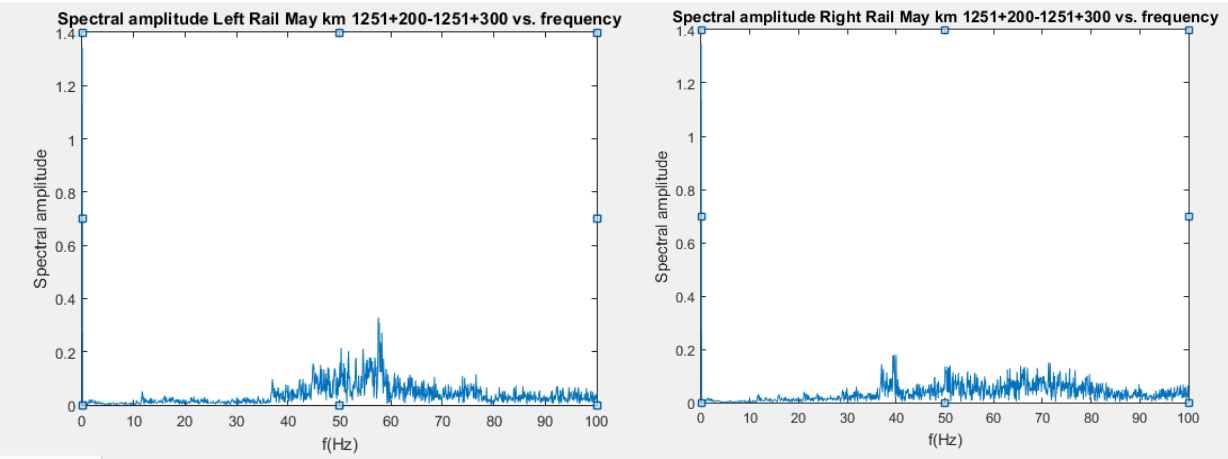

Figure 29. Results of frequency analysis between 0-100 Hz, Polcirkeln-Koskivaara km 1251+200-1251+300 May 2016.

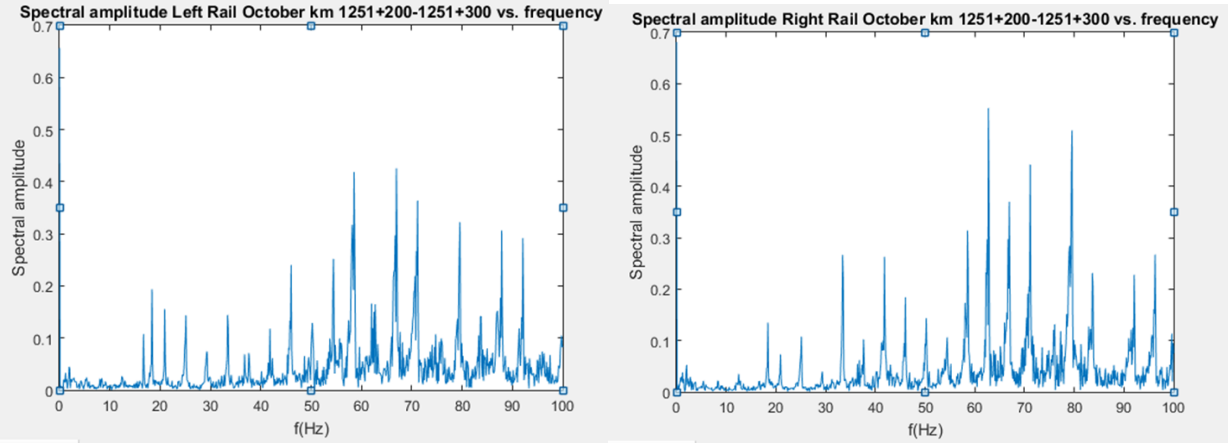

Figure 30. Results of frequency analysis between 0-100 Hz, Polcirkeln-Koskivaara km 1251+200-1251+300 October 2016.

Results of the FFT on the signals from km 1251+200-1251+300 for frequencies between 100 and 450 Hz, where other components eigenfrequencies emphasize more.

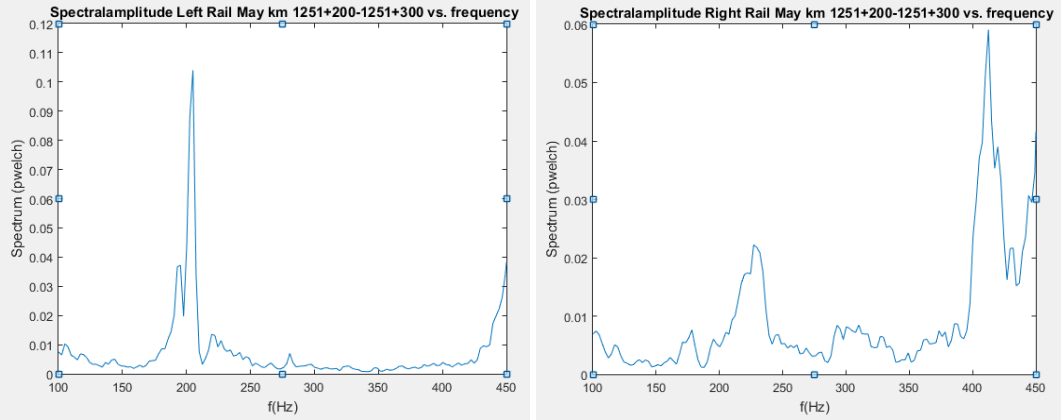

Figure 31. Results of frequency analysis between 100-450 Hz, Polcirkeln-Koskivaara km 1251+200-1251+300 May 2016.

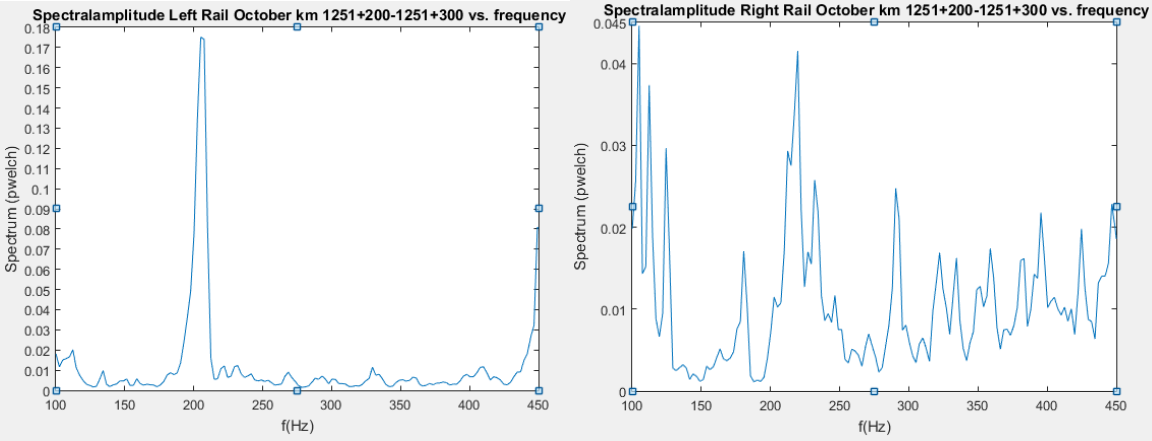

Figure 32. Results of frequency analysis between 100-450 Hz, Polcirkeln-Koskivaara km 1251+200-1251+300 October 2016.

Results of the FFT on the signals from km 1251+200-1251+300 for frequencies up to 2500 Hz, where other components eigenfrequencies emphasize more.

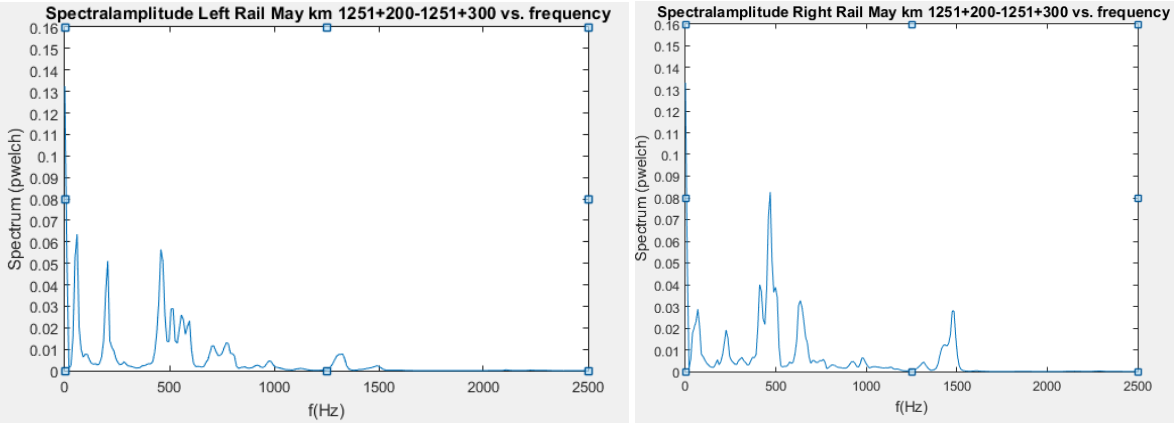

Figure 33. Results of frequency analysis between 0-2500 Hz, Polcirkeln-Koskivaara km 1251+200-1251+300 May 2016.

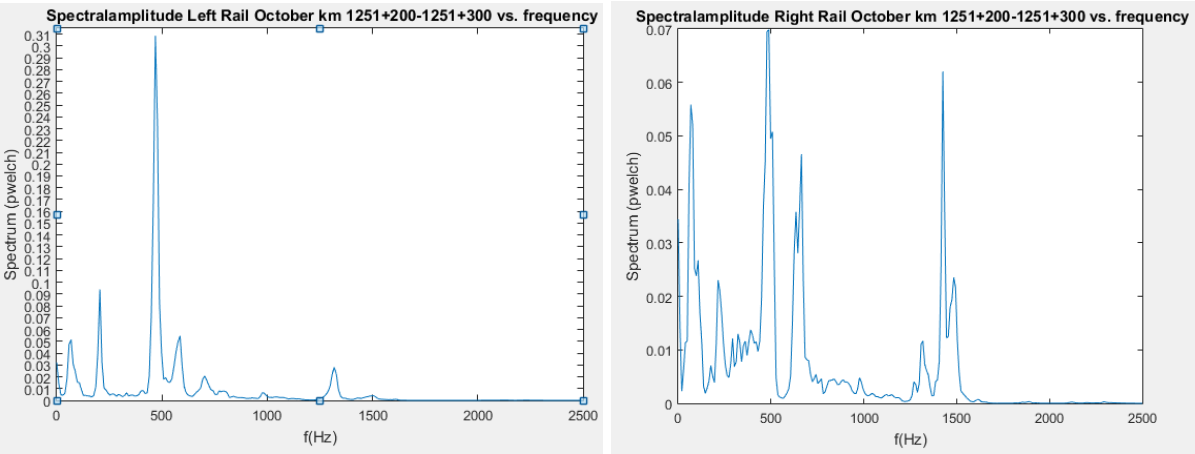

Figure 34. Results of frequency analysis between 0-2500 Hz, Polcirkeln-Koskivaara km 1251+200-1251+300 October 2016.

5 Analysis

5.1.1 Tolikberget km 1222+300-1222+400

Weather conditions during the thawing period in May are important to know, because it shows whether the covering snow layer is still left or not. Which determines to some extent the subsoils degree of saturation and if the subsoil might still be frozen. The closest material available from the film database for determination of the weather conditions is from May 16th 2016. According to the material (Trafikverket, Järnvägsfilm Bandel 118 , 2016) the weather conditions are dry at the surface, because, the ground surface is not covered by snow (Figure35). Due to the altitude where Tolikberget is located, which is in the northern part of Sweden, the subsoil might still be frozen to some extent. Thus, the subsoil could be more water saturated.

During the measurements, the trains have travelled with different speed, but the difference is small seen in percentage. Therefore, it is appropriate to assume, that in this case the trains speed does not have any significant influence on the results.

Figure 35. Weather conditions along Tolikberget km 1222+300-1222+400, 16 of May 2016. (Trafikverket, Järnvägsfilm Bandel 118 , 2016)

5.1.2 Analysis of measurements in May, Tolikberget km 1222+300-1222+400

From the results obtained from measurements in May resonance frequencies associated to all parts of the railway superstructure and the subsoil can be detected. The lowest resonance frequency is about 4 Hz, which can be related to the sleepers according to section 2.2.1.

At 24 Hz, an amplification can be detected, which probably is related to the subsoil. Since, according to the calculations of expected eigenfrequency of the subsoil the value should be around 26 Hz. Another resonance frequency which occurs and can be related to the subsoil, is the frequency of 35 Hz, since according to (Figure 5) the eigenfrequency of coarse grained soils can as well be a bit higher than the one obtained from calculations.

The ballast layer has an expected eigenfrequency of about 120 Hz, and peaks around this frequency are possible to detect, therefore are they most likely related to the ballast.

According to section.2.2.3 the eigenfrequency of a superstructure with concrete or wooden sleepers is between 44 and 49 Hz. At 47 Hz amplifications can be detected, therefore, it is reasonable to relate this to the superstructure.

Between 60-90 Hz several amplification peaks occur, and according to section.2.2.2 resonance frequencies in this range can be related to the track grid, therefore, it is appropriate to do so in this case.

In the higher frequency range, between 250 and 400 Hz several peaks can be detected. These peaks are according to section.2.1 related to rutting ripples.

The so called pinned-pinned frequencies, which have an eigenfrequency of 1000 Hz are possible to detect in the measurements in May but not in October. This might have a connection with a softer soil condition in May, due to the thawing.

5.1.3 Analysis of measurements in October, Tolikberget km 1222+300-1222+400

The results obtained from October measurements are in general similar to ones from May. Basically, the difference is, that from measurements in May the amplification of the subsoil eigenfrequency at 24 Hz is about two times higher for the left rail compared to the right rail. But for the measurements in October, the situation is the opposite. The reason for this is either connected to soft soil conditions due to thawing in May and the drier conditions in October. Or there has been performed measurements from the other direction in one of the measurements without being labelled.

There is as well a difference between May and October in the amplification of pinned-pinned frequencies. In October, a minor amplification can be detected at 1000 Hz compared to the magnitudes in May. Which may be due to drier conditions in October.

5.1.4 General analysis of resonance impact on subsoil and ballast Tolikberget km 1222+300-1222+400

By the investigations performed by (Noppa, 2003), the groundwater table is located below the ballast layer. This implies that the subsoil conditions are wet, therefore, when the subsoil is affected by resonance due to dynamic loading, which is the case along Tolikberget, a risk for liquefaction arises according to (Richart & Woods, 1970) pp.172-174. In addition, this phenomenon will lead to a reduction of the soils shear strength and the soil loses its bearing capacity which will cause settlements on the railway embankment. But there can as well arise a liquefaction of the ballast layer, if the pore pressures are high enough to cause the water to move upwards through the ballast.

Even if the subsoil would be in dry conditions, it would be affected by dynamic loading, and according to (Richart & Woods, 1970) pp.180-182 the permanent vertical strains increases for cohesionless soils with increasing number of load cycles. Therefore, it is important to consider all situations where the soil gets into resonance.

According to (Angerhn, 2015) the impact of dynamic loading on ballast causes deterioration of the material. Which in origin stage is of square and angular shape, but with time a formation to rounder grains will take place. This causes a decrease of the dilatancy angle, which leads to a contraction (settlement) of the ballast bed. As well a rise of fine grained material between the larger grains occur, therefore, a degradation of the shear strength, shear modulus as well as the bearing capacity of the ballast occur.

5.2.1 Polcirkeln-Koskivaara km 1251+200-1251+300

Available material for Polcirkeln-Koskivaara in the film database (Trafikverket, Järnvägsfilm Bandel 118 , 2016) is just a little bit before km 1251+200-1251+300 and after, from the period in May 2016 (Figure36). Along this section during this period, there is no covering snow layer left. But due to the altitude of this section, which is in the northern part of Sweden, the subsoil is still most likely frozen to some extent. Which must be considered further in the analysis.

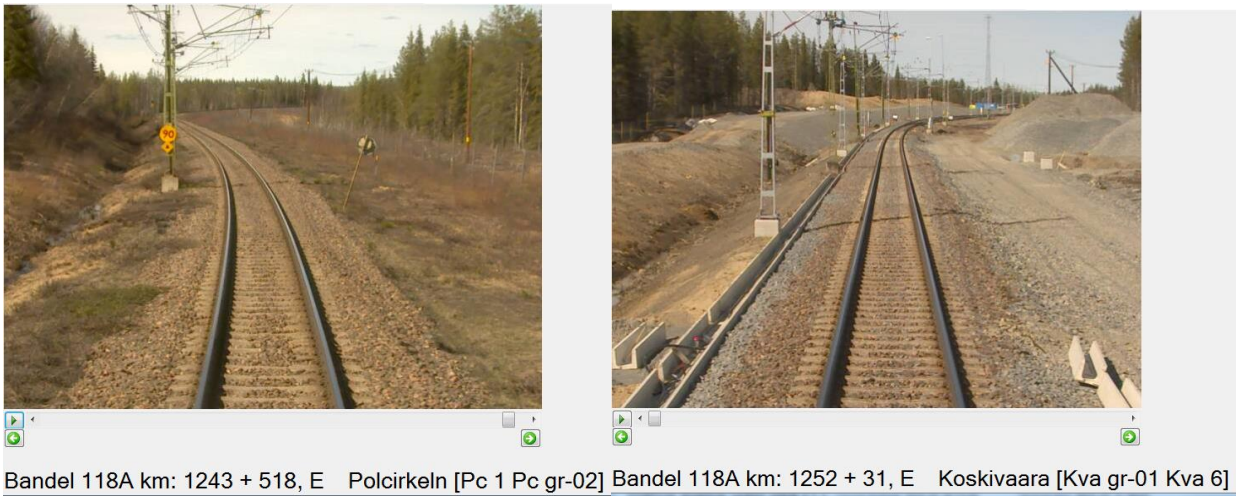

Figure 36. Weather conditions along Polcirkeln-Koskivaara, 16 of May 2016. (Trafikverket, Järnvägsfilm Bandel 118 , 2016)

5.2.2 Analysis of measurements in May, Polcirkeln-Koskivaara km 1251+200-1251+300

The results of these measurements indicate that there is a deviation from the expected. Since the signals does not show greater variations in the amplitudes between 0 and 100 Hz. Explanation for this is either, that the trains speed in May is in percentage much lower than it is in October. Or that the subsoil is still frozen to some extent, which means that there is more or less a layer of ice due to the high water content in peat. Which implies that a layer of ice contributes to resonance peaks at much higher frequencies than for soils, since according to (Kohnen, 1974) the shear wave velocity for ice is about 1950 m/s. Therefore, if the thickness of the ice layer is between 0.5m and 1m, then the eigenfrequency of ice is between 487.5 and 975 Hz. By the results, it is possible to detect amplifications of very high frequencies, but more detailed research must be done before these resonance peaks can be with accuracy related to ice. Since peaks at similar frequencies are possible to detect in the results in October.

Resonance frequencies which can be detected primarily in the range of 0-100 Hz is, 40-45 Hz and 50-57 Hz. The frequencies of these two resonance ranges are most likely related to the superstructure. Since the expected eigenfrequency of the superstructure according to section.2.2.3 is between 44-49 Hz and due to the calculations in section.4.2.2 the ballast has an eigenfrequency of 44.5 Hz with a layer thickness of 1.5 meters or a bit higher if the thickness of the ballast layer decreases. As well as these frequency ranges only corresponds to the higher range of possible eigenfrequencies of peat and in the results, there is missing all possible low resonance frequencies of peat.

5.2.3 Analysis of measurements in October, Polcirkeln-Koskivaara km 1251+200-1251+300

These results from October measurements, shows a clear difference in the range 0-100 Hz compared to the results in May. Resonance frequencies for peat are possible to detect from the lower range up to the higher range. Which is positive due to the wide range of possible eigenfrequencies that is expected for peat from the calculations.

In these results, amplifications occur in the same ranges as in May, which then confirms that frequencies between 40 and approximately 57 Hz is related to the ballast layer. There are as well resonance frequencies in the range of 60 – 90 Hz, which are according to section.2.2.2 related to the track grid.

From the right rails results, it is possible to distinguish clearer compared to those from May, that there occur amplifications in the range for rutting ripples (250-400Hz).

5.2.4 General analysis of resonance impact on subsoil and ballast Polcirkeln-Koskivaara km 1251+200-1251+300

Since the subsoil consists of peat with a high water content, it is clear that the soil is more or less in a liquid state. Therefore, when the peat is affected by resonance due to dynamic loading, the pore pressure increases. Which in turn can cause the water to move upwards and probably through the ballast layer, where a second state of liquefaction can arise.

When considering the resonance of the ballast layer only, according to (Angerhn, 2015) there occur as described earlier, a deterioration of the material. Which in origin stage is of square and angular shape, and by time the shape becomes round. This causes a decrease of the dilatancy angle, which leads to a contraction (settlement) of the ballast bed. As well as an increase of the amount of fine grained material between the larger grains. Which causes a degradation of the shear strength, shear modulus as well as the bearing capacity of the ballast.

5.3 Stationary measurements from Notviken

The measurements performed at the rail (Appendix 3) provides noisy signals which leads to difficulties when it comes to the analysis. Since it is hard to distinguish any specific frequencies due to the amount of noise.

From the sleeper measurement (Appendix 3) it is possible to detect amplifications between 0-150 Hz, which can with a great certainty be related to subsoils and ballast layers. As well as there are amplifications in the range for rutting ripples (250-400 Hz), where a clear resonance can be detected at 400 Hz.

6 Discussion

Considering this analysis method, it becomes interesting when the expectations correlates with the analysis results. Therefore, a good indication is obtained that this method is reliable and useful. By this, questions arise about the long term use of frequency analysis. One answer for this could be, that the amount of site investigations in the form of borehole sampling can be reduced. Since when the soil conditions for one section is known, there is then possibilities to investigate the magnitude of impact on the soil due to dynamic loading by frequency analysis. As well as an estimation of the consequences on the soil can be performed.

Another possible use of this analysis method could be to follow up the conditions along a railway or roadway. Therefore, it would be a nice way to investigate how the impact on the soil varies between different seasons during the year as well as for variations in the speed of the train/vehicle. Which would be of help to understand when and where different actions needs to be taken.

When considering the analysis of measurements from Tolikberget and Polcirkeln-Koskivaara, differences in the results are possible to see due to the season or speed. The differences in spectral amplitude between the different measurements are of course of interest, since these indicates how big the differences are regarding the impact. Where the reason for it is of interest as well, because it can be due to variations in water content, thickness of ice layer and degree of compaction.

Then appears the impact on the other components as well belonging to a railway superstructure. Where some parts are more of interest for railway maintenance people, like the rails and sleepers, and how they are affected by the dynamic loading.

A comparison between measurements obtained from trains and stationary accelerometers. Indicates that same type of information should be possible to obtain from stationary accelerometers, especially from one that is mounted on a sleeper. Therefore, this observation provides the interesting result that these measurements can be performed in different ways but still have the ability to get the desired information.

Considering the analytical calculations of expected eigenfrequencies, the accuracy of the obtained values is of course possible to improve. Because with lab testing of current soil samples, where the shear modulus and density of the soil would be determined. More accurate calculations of the expected eigenfrequencies could be performed. Another factor which would contribute to the accuracy is current borehole sampling. Then, current soil layer information for the calculations would be achieved.

The precision of acceleration measurements regarding the location along the railway where the measurements are pointed out to be in the datafile, could be a subject for improvement. Since the measurements are not fully automated, there is probably in every measurement an error regarding the human factor. Which means that the measurements location will not exactly be at the position where it is pointed out to be in the data file. Because the measurements must be started manually when the train is moving, which causes delays.

7 Conclusions

It is definitely possible to determine that this is an analysis method that provides information and knowledge about how the dynamic loading affect the railway embankment and subsoil. This method still depends on other soil investigations, but the amount of other expensive soil investigations should be possible to reduce. Since, the impact on ballast or subsoil can be verified with frequency analysis along a longer part of a section, without taking soil samples at frequent intervals.

There are possibilities to use this method for other purposes as well. For example, if one could determine the magnitudes and frequency ranges of the railway traffic along a section, then it could be used for design of the railway embankment, to minimize the negative impacts from railway traffic.

This method can be used for back calculation of soil layer thicknesses. Because, if the soil type is known for a section, then by interpretation of the frequency obtained from measurements into the analytical equation, the thickness is possible to obtain. This is of special importance to old tracks where little or no documentation exists about the ground and the design has been adapted empirically.

The results from the analysis, shows that the theoretical calculations correlate with the measured values. Which is of importance for verification of this analysis method.

For the two analysed sections, the most critical consequence is the development of liquefaction, since it causes loss in bearing capacity for the soil and ballast, which leads to settlements. The other consequence which is something that a ballasted railway always must deal with, is the deterioration of ballast due to dynamic loading. But with knowledge of the railway traffics magnitude and frequency range, the size of the impact on ballast can reduced, by changes in the ballast layer thickness, which determines its eigenfrequency. Therefore, it would be of importance to achieve a stable subsoil which does not cause settlements, to be able to reduce the impact on ballast by having the right layer thickness.

Considering the soil conditions along Tolikberget where the groundwater table is high and the railway embankment is subjected to long ore trains, which implies that liquefaction can occur in the subsoil and ballast. Therefore, by measurements of the accelerations on the sleepers one could detect the onset of liquefaction.

To reduce the occurrence of liquefaction along Tolikberget, a drainage of the embankment could be one possible measure to take.

Since the railway traffic, speed and weight of the trains most likely will increase along the Swedish railway network. An inevitable detail regarding the design of railway embankments in the future, is the consideration of dynamic loading.

8 Future work

Proposals for future work in this area for coming master thesis could be:

- Compare in detail measurements performed by trains and stationary accelerometers
- Follow up measurements from several years for one section, where the aim is to estimate the reason for the differences
- Compare the development of compaction with changes of the ballast eigenfrequency for a new railway embankment
- Estimate the layer thicknesses in the subsoil by frequency analysis
- Perform frequency analysis on a roadway section, where the accelerometer would be mounted on a heavy truck

References

Angerhn, F. (2015). *Frequenzanalyse von Achslagerbeschleunigungen. Masterarbeit Studiengang Bauingenieurwissenschaften, Eidgenössische Technische Hochschule Zürich, Swiss Federal Institute of Technology Zürich.*

Axelsson, K., & Mattsson, H. (2016). *Geoteknik.* Lund: Studentlitteratur.

Grip, N. (2017, February 2). Verification of Matlab code. (J. Majala, Interviewer)

Gripner, S. (2012). *Optram presentation, Trafikverket*. Retrieved from <http://www.trafikverket.se/optram> 11 November 2016

Gustafsson, S., Engström, T., & Finnberg, Ö. (2016). *MUR-GEOTEKNIK, Förstärkningsåtgärder km 1250+980-1251+400, Bandel 118 Polcirkeln-Koskivaara.* Trafikverket Investering Nord.

Kohnen, H. (1974). The Temperature dependence of seismic waves in ice. *Journal of Glaciology, Vol.13, No.67*, 4.

Larsson, R. (2008). *Jords egenskaper, Statens Geotekniska Institut*. Retrieved from <http://www.swedgeo.se/globalassets/publikationer/info/pdf/sgi-i1.pdf> 26 April 2017

Lekarp, F., Isacsson, U., & Dawson, A. (2000). Permanent Strain Response of Unbound Aggregates. *Journal Of Transportation Engineering. pp.76-79.*

Lichtberger, B. (2005). *Track compendium : formation, permanent way, maintenance, economics.* Hamburg: Eurailpress.

MathWorks. (2017a). *Fast Fourier Transform Matlab*. Retrieved from <https://se.mathworks.com/help/matlab/ref/fft.html?s_tid=gn_loc_drop> 23 January 2017

MathWorks. (2017b). *Welch's power spectral density estimate*. Retrieved from <https://se.mathworks.com/help/signal/ref/pwelch.html> 27 January 2017

Noppa, J. (2003). *PM Geoteknik, BANDEL 118, Boden-Gällivare, BANSTRÄCKA: Näsberget-Murjek, Ny Mötestation vid Tolikberget.* Banverket Projektering.

Profillidis, V. (2007). *Railway Engineering.* Aldershot, Burlington, USA: Ashgate.

Richart, F., & Woods, R. (1970). *Vibrations of soils and Foundations.* Prentice-Hall, Inc.Englewood Cliffs, New Jersey.

Serridge, M., & Licht, T. (1987). *Pietzoelectric accelerometer and vibration preamplifier handbook.* Glostrup Denmark: K Larsen & Sön A/S.

Storey, B. D. (2017). *Computing Fourier Series and Power Spectrum with MATLAB, Source <http://faculty.olin.edu/bstorey/Notes/Fourier.pdf> 3 February 2017. pp.1-7.*

Studer, J. A., Laue, J., & Koller, M. G. (2007). *Bodendynamik.* Berlin Heidelberg: Springer-Verlag.

Towhata, I. (2008). *Geotechnical Earthquake Engineering.* Berlin, Germany: Springer-Verlag.

Trafikverket. (2011). *TK Geo 11, Trafikverkets tekniska krav för geokonstruktioner, Trafikverket.* Retrieved from <https://trafikverket.ineko.se/Files/sv-SE/10749/RelatedFiles/2011_047_tk_geo_11_2.pdf> 26 April 2017

Trafikverket (Director). (2012). *Järnvägsfilm Bandel 118* [Motion Picture].

Trafikverket (Director). (2016). *Järnvägsfilm Bandel 118* [Motion Picture].

Trafikverket. (2017). *Geoteknisk Databas*. Retrieved from <http://ppikarta4.trafikverket.se/GeoArkivMap.aspx?MapId=a28ebb04-17b7-4f31-b938-9077f421a179&export=1> 19 April 2017

Trafikverket. (2017). *Malmbanan,Trafikverket* . Retrieved from <http://www.trafikverket.se> 7 April 2017

Trafikverket. (2017, 03 17). ProjectWise Explorer V8i. *Förvaltningsdata,Banunderbyggnad/Banöverbyggnad,Geoteknik,Norr*. Luleå.

Vibrationdata. (2017, 01 16). *Vibrationdata El Centro Earthquake*. Retrieved from < http://www.vibrationdata.com/elcentro.htm > 16 January 2017

Appendix

Appendix 1 Length sections for Tolikberget

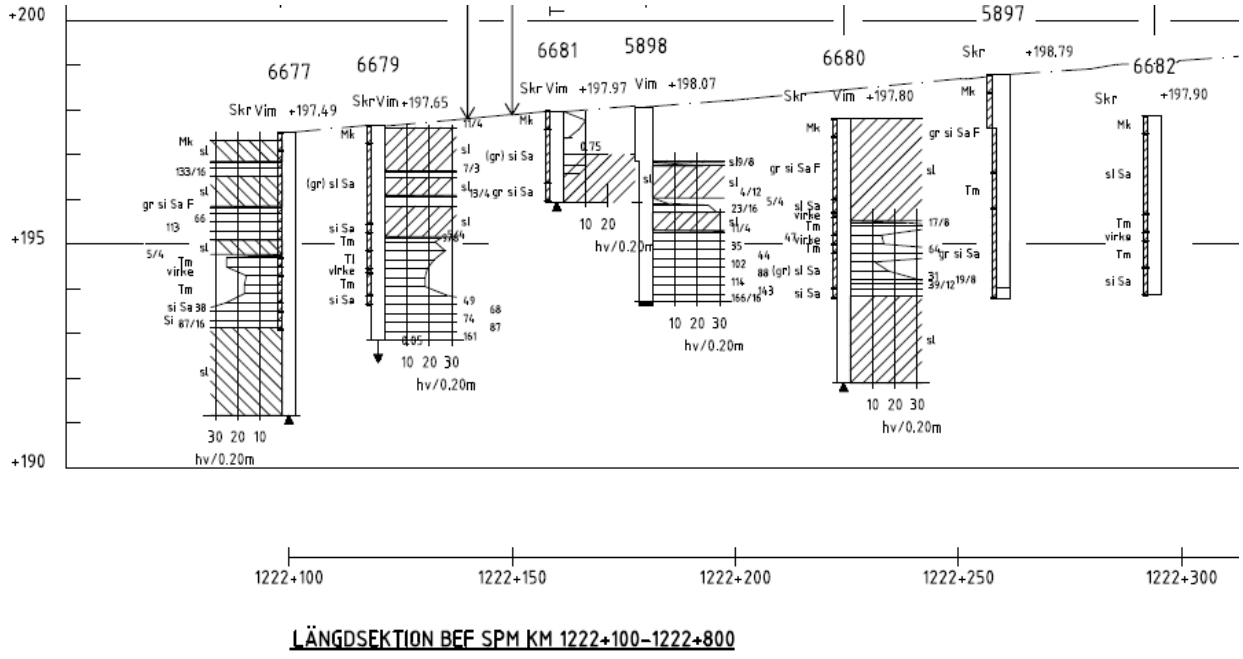

Figure 37. Length section for Tolikberget km 1222+100-1222+300. (Trafikverket, ProjectWise Explorer V8i, 2017)

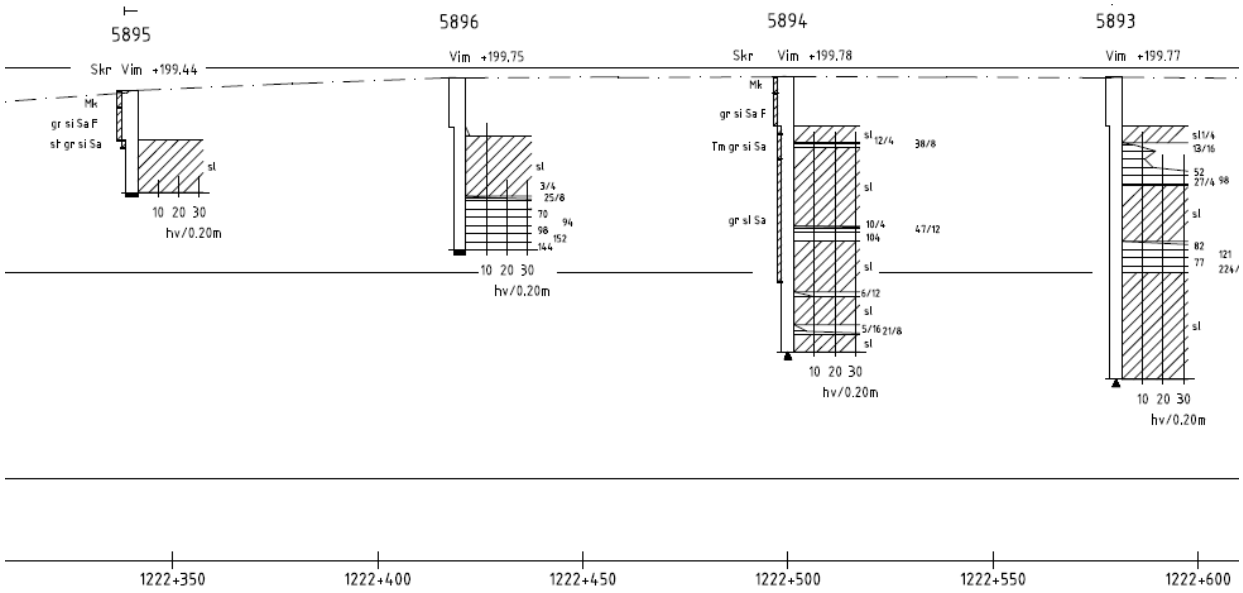

Figure 38. Length section for Tolikberget km 1222+350-1222+600. (Trafikverket, ProjectWise Explorer V8i, 2017)

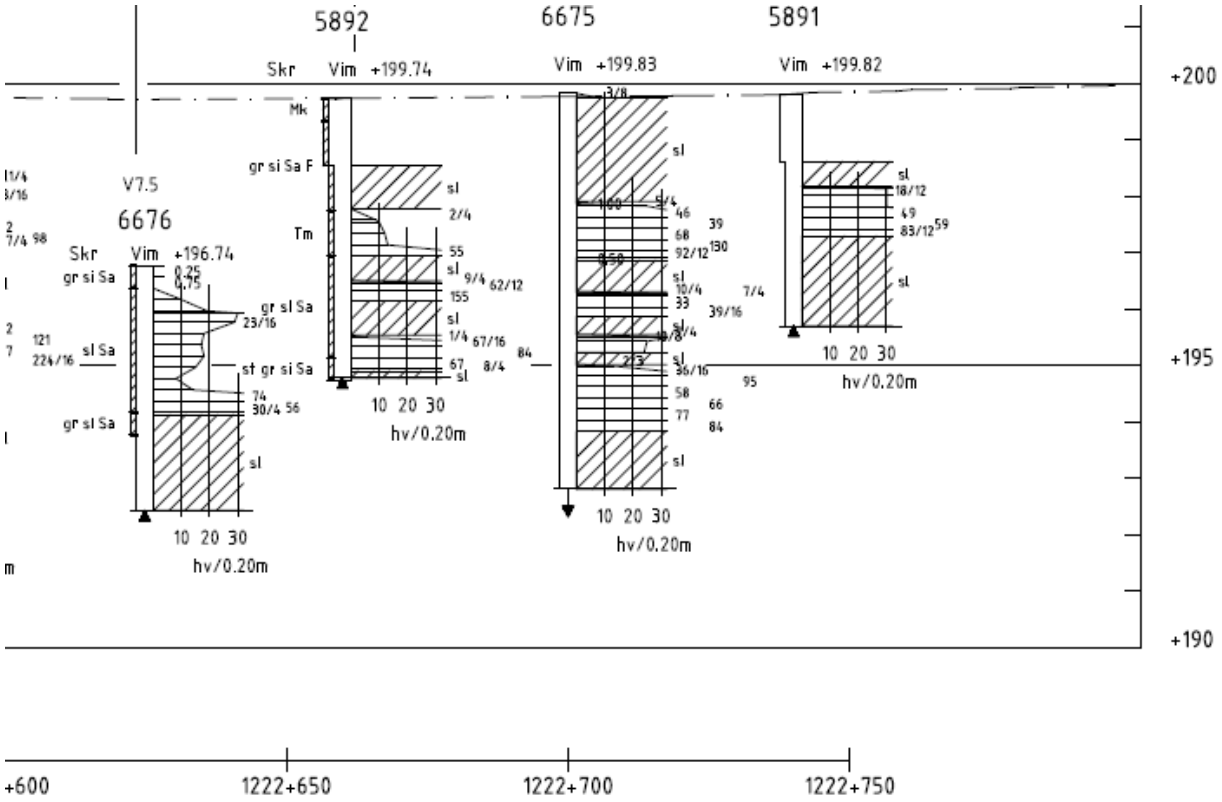

Figure 39. Length section for Tolikberget km 1222+600-1222+750. (Trafikverket, ProjectWise Explorer V8i, 2017)

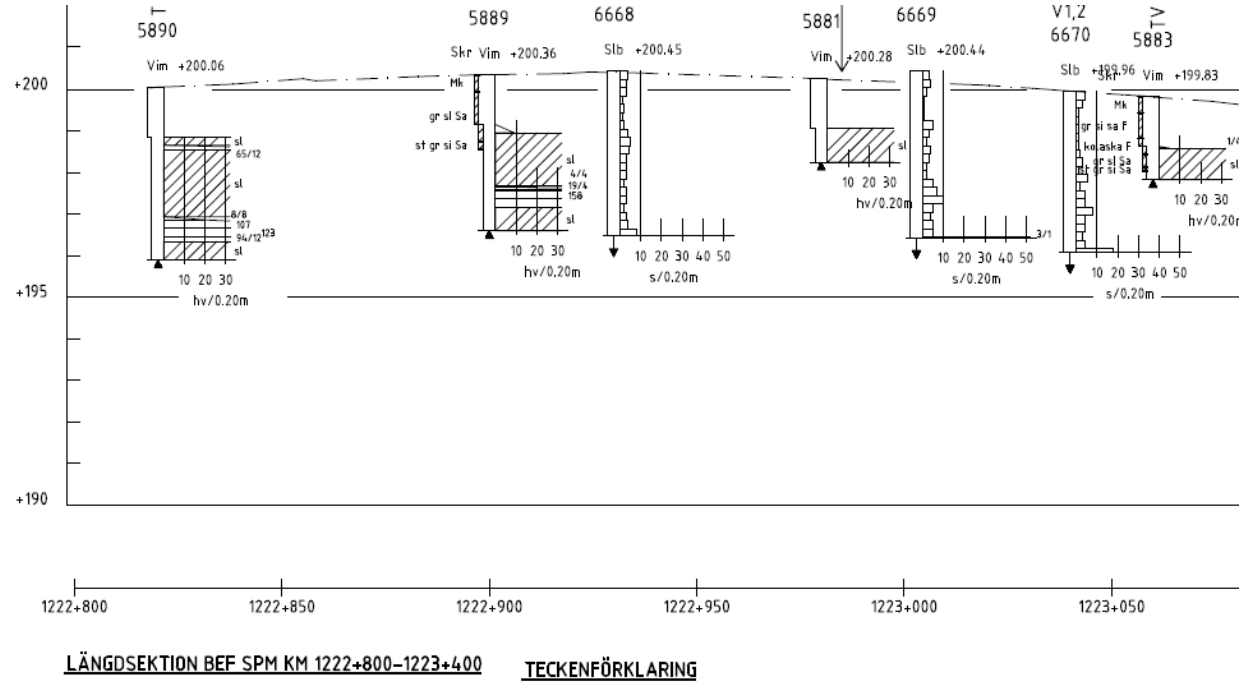

Figure 40. Length section for Tolikberget km 1222+800-1223+050. (Trafikverket, ProjectWise Explorer V8i, 2017)

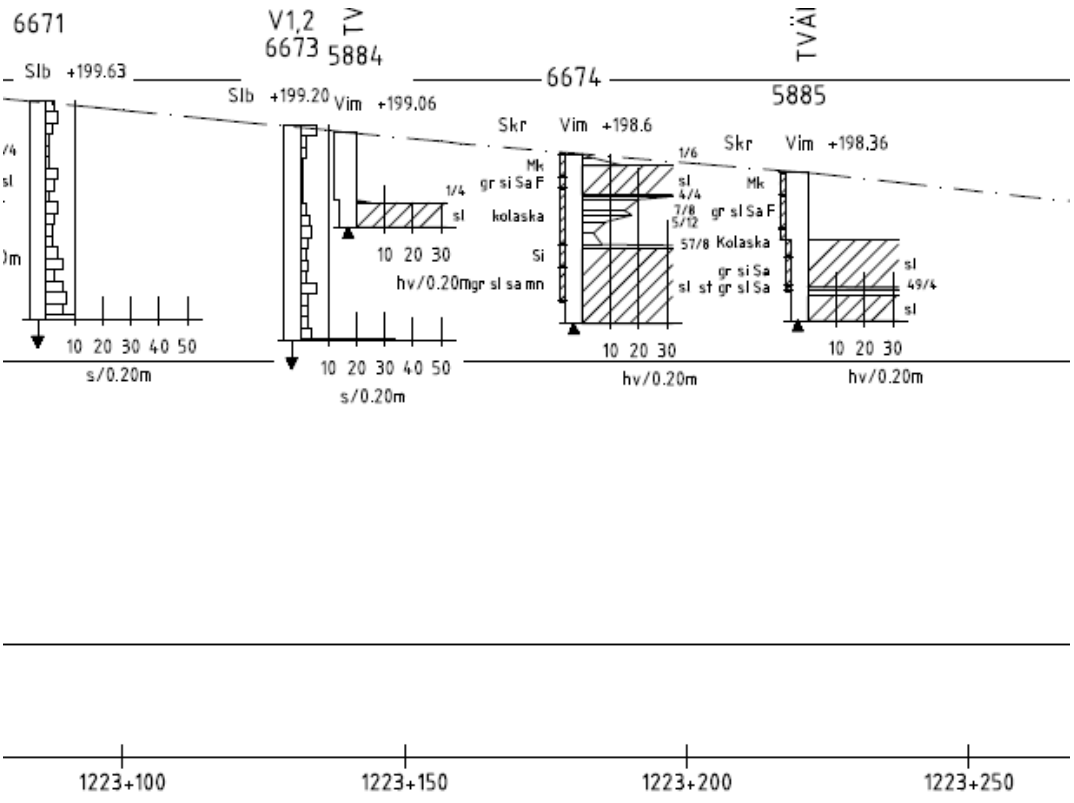

Figure 41. Length section for Tolikberget km 1223+100-1223+250. (Trafikverket, ProjectWise Explorer V8i, 2017)

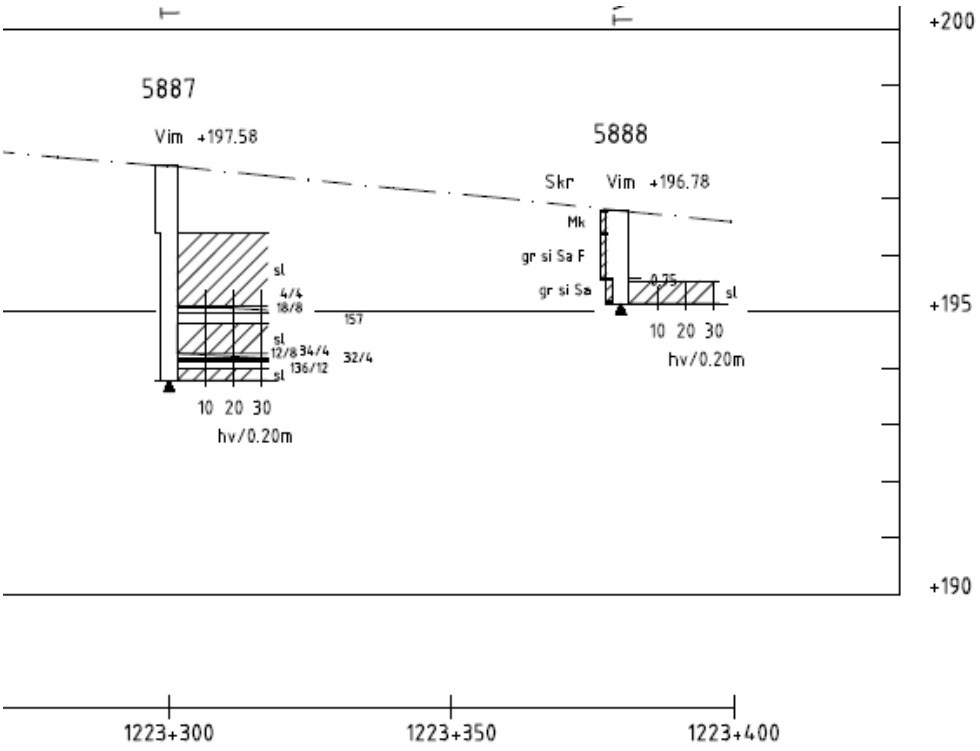

Figure 42. Length section for Tolikberget km 1223+300-1223+400. (Trafikverket, ProjectWise Explorer V8i, 2017)

Appendix 2 Matlab coding

Appendix 2.1. Fast Fourier Transformation code for Matlab

```
Fs = 50; % Sampling frequency
T = 1/Fs; % Sampling period
L = 2688; % Length of signal
t = (0:L-1)*T; % Time vector
X = ElcentroNS(:,1); % Peak ground acceleration vector
Y = fft(X); % Fourier transform of the signal
P2 = abs(Y/L); % Two-sided spectrum P2
P1 = P2(1:L/2+1); % Single-sided spectrum P1
P1(2:end-1) = 2*P1(2:end-1);
f = Fs*(0:(L/2))/L; % Frequency
plot(f,P1)
title('ElcentroNS spectral amplitude vs. frequency')
xlabel('f(Hz)')
ylabel('Spectral amplitude')
```

Figure 43. Fast Fourier Transformation code for Matlab.

Appendix 2.2. Noise reduction code for Matlab

```
>> %[Yw,fw]=pwelch(X,[],[],250);
winLen=500; % Split signal in segments of this lenght
winOverlap=250; % Number of samples overlap between segments
%f=
[Yw,fw]=pwelch(X,winLen,winOverlap,[],Fs);
figure(4)
plot(fw,Yw);
title('ElcentroNS Spectralamplitude vs. frequency')
xlabel('f(Hz)')
ylabel('Spectrum (pwelch)')
```

Figure 44. Noise reduction code for Matlab.

Appendix 3 Rail & Sleeper frequencies Notviken

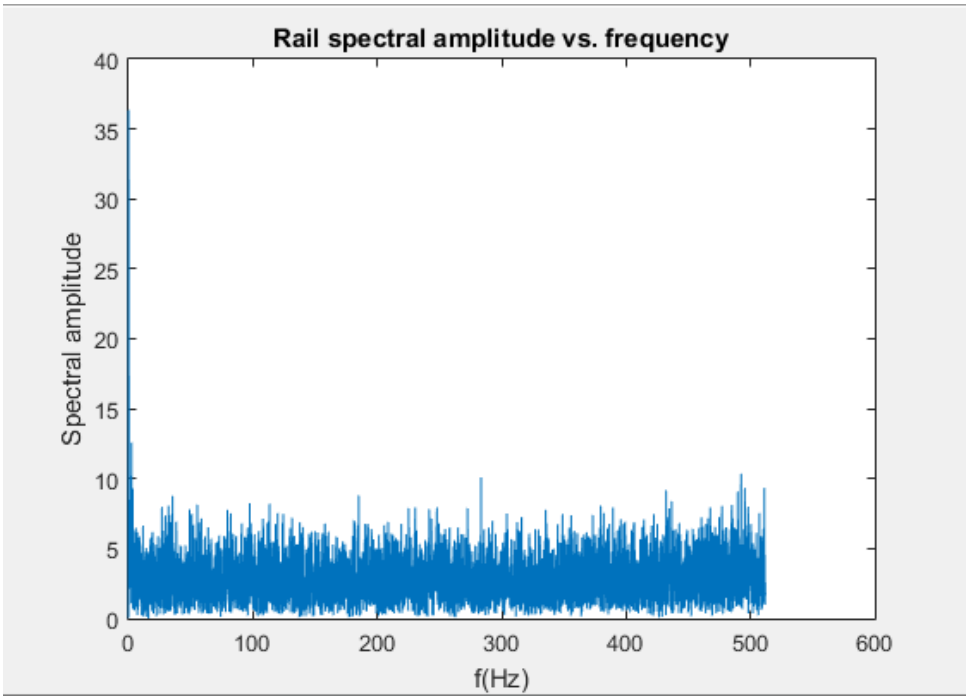

Figure 45. Results from measurements at the rail.

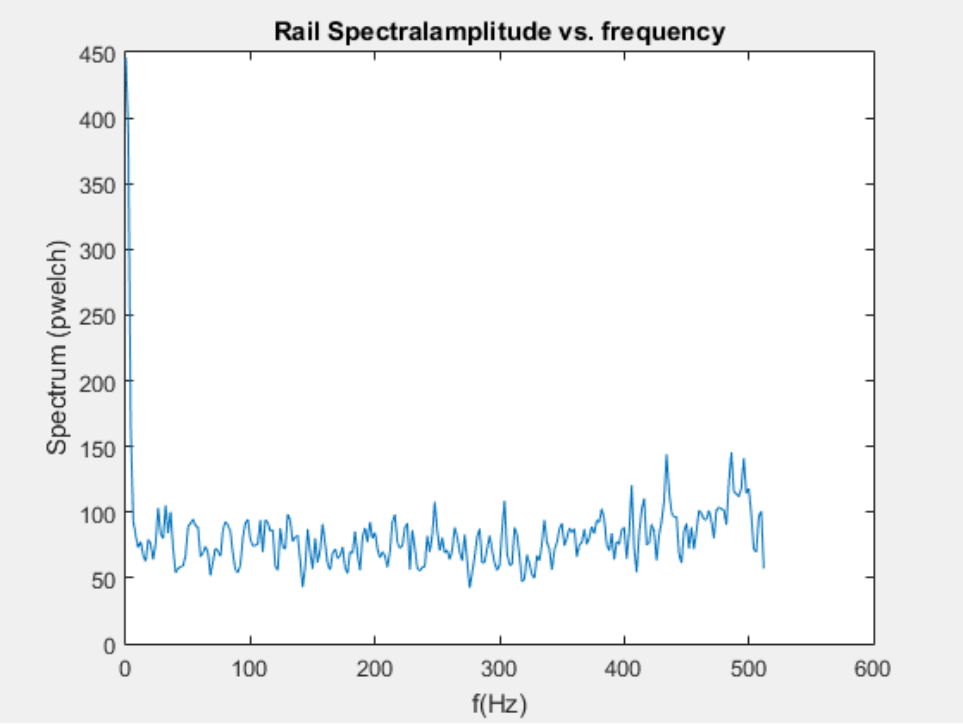

Figure 46. Noise reduced results from measurements at the rail.

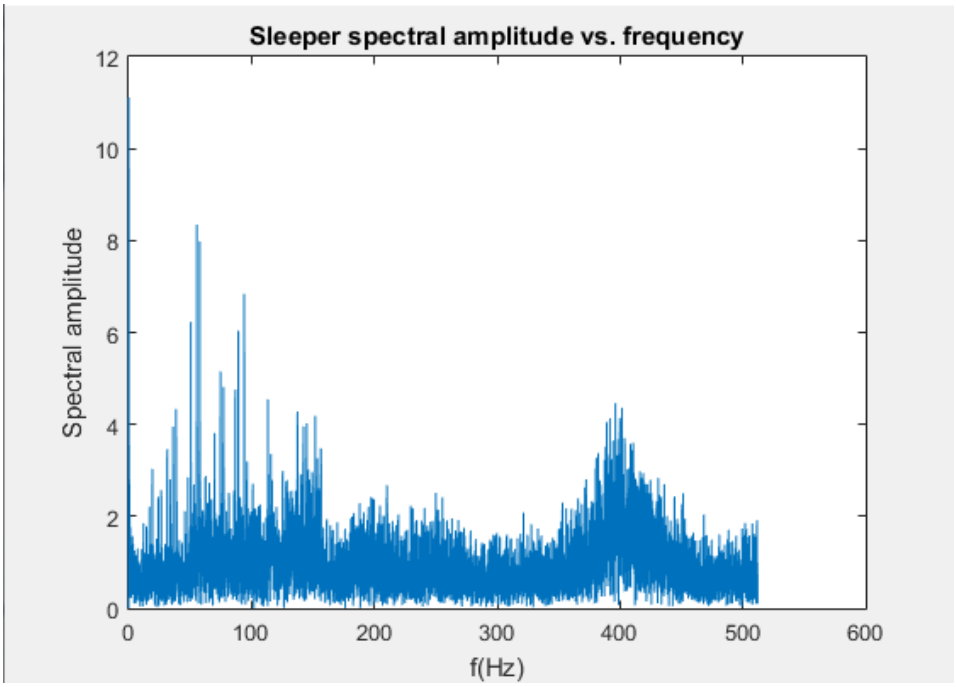

Figure 47. Results from measurements at the sleeper.

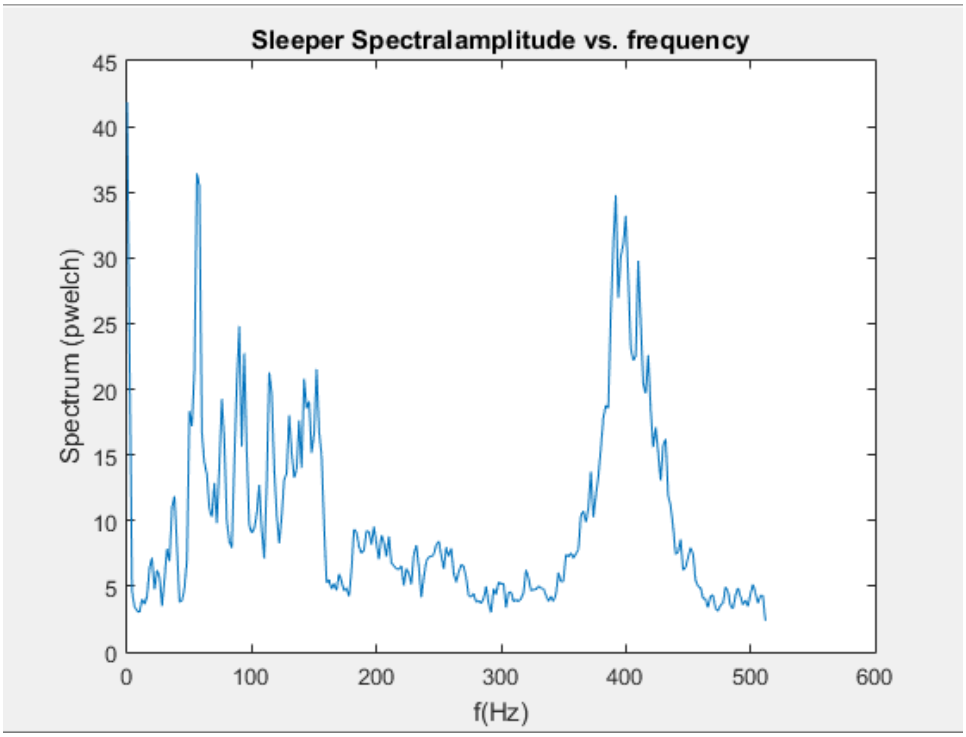

Figure 48. Noise reduced results from measurements at the sleeper.

Appendix 4 Calculations of expected eigenfrequencies, Tolikberget

4.1 Expected eigenfrequency of subsoil

For determination of the subsoils eigenfrequency equation (4.1) is used, this in turn implies that three parameters must be known, namely the shear modulus, the subsoils density and the thickness of the soil layer. A compendium about soil properties from Swedish Geotechnical Institute gives information of the densities of different soil types (Larsson, 2008). Therefore, in this case when the subsoil lies underneath the ground water table, the water saturated density is derived from the water saturated heaviness of the subsoil. The heaviness for gravely silty sand is calculated by taking the sum of the values for each soil type and then divide the sum by three.

Water saturated heaviness of various soils, γ_w:

Gravel: $\gamma_w = 22$ kN$/m^3$

Silt: $\gamma_w = 19$ kN$/m^3$

Sand: $\gamma_w = 20$ kN$/m^3$

Water saturated heaviness of gravely silty sand, γ_w:

$$\gamma_w = \frac{22+19+20}{3} = 20.33 \text{ kN}/m^3$$

When the heaviness is known, the density is easily derived by a division of the heaviness with the gravitational acceleration, g. Thus, the water saturated density of gravely silty sand is

$$\rho_w = \frac{\gamma_w}{g} = \frac{20.33}{10} = 2.033 \ {}^{t}/_{m^3} = 2033 \ {}^{kg}/_{m^3}$$

The shear modulus is determined according to Trafikverkets technical requirements for geotechnical constructions TK Geo 11 (Trafikverket, TK Geo 11, Trafikverkets tekniska krav för geokonstruktioner, Trafikverket, 2011). According to this document the initial shear modulus must be reduced in accordance with the actual shear strains within the soil. But in this case the initial shear modulus must be used for calculations of the soils eigenfrequency as this is based on the wave velocities. (Studer et.al)

The equation for determination of initial shear modulus for coarse grained material according to (Trafikverket, TK Geo 11, Trafikverkets tekniska krav för geokonstruktioner, Trafikverket, 2011) is

$$G_0 = K_1 * (\sigma'_m)^{0.5} \qquad (8)$$

Where K_1 is a constant which is dependent of the material and degree of compaction. The value varies between 15000 and 30000, the higher value is related to crushed material like ballast and the lower one is related to sand. For this case, a K_1 value of 21000 is assumed to be reasonable.

The mean effective stress σ'_m is calculated in two dimensions, which means that σ'_m is composed of a vertical effective stress σ'_v and horizontal effective stress σ'_h. According to (Axelsson & Mattsson, 2016) the horizontal effective stress σ'_h is equal to $K_0 * \sigma'_v$. Where K_0 is the lateral earth pressure coefficient and for well compacted sand it has a value of 0.35, which

is a valid value to use in this case. Since the railway embankment and its subsoil has been affected by heavy traffic for a long time. The mean effective stress is then calculated as, $\sigma'_m = \frac{\sigma'_v+\sigma'_h}{2}$, (Axelsson & Mattsson, 2016). For vertical effective stress calculations, the effective heaviness is used, since the subsoil is underneath the ground water table. Therefore, according to (Larsson, 2008) the effective heaviness for gravel, silt and sand is:

Gravel: $\gamma' = 12$ kN$/m^3$

Silt: $\gamma' = 9$ kN$/m^3$

Sand: $\gamma' = 10$ kN$/m^3$

Thus, the effective heaviness for gravely silty sand is, $\gamma' = \frac{12+9+10}{3} = 10.33$ kN$/m^3$

But in this case when calculating the vertical effective stress, the weight of the ballast must be added. The ballast layer is above the ground water table, which implies that the heaviness of natural moisture ballast is relevant to use, where $\gamma' = 18$ kN$/m^3$ for the ballast. Thereby the vertical and horizontal effective stresses are calculated for this soil stratigraphy as follows:

$\sigma'_v = \gamma'_{Ballast} * z + \gamma'_{Gravely\ Silty\ Sand} * z = (18 * 0.4) + (10.33 * 2) = 27.86$ kN$/m^2$

$\sigma'_h = K_0 * \sigma'_v = 0.35 * 27.86 = 9.751$ kN$/m^2$

By this the mean effective stress is, $\sigma'_m = \frac{\sigma'_v+\sigma'_h}{2} = \frac{27.86+9.751}{2} = 18.81$ kN$/m^2$

The shear modulus is then, $G_0 = K_1 * (\sigma'_m)^{0.5} = 21000 * (18.81)^{0.5} = 91078$ kN$/m^2$

Thus, according to equation (4.1) the eigenfrequency of the gravely silty sand layer is,

$$f_0 = \frac{v_s}{4H} = \frac{\sqrt{G/\rho_w}}{4H} = \frac{\sqrt{91078*10^3/2033}}{4*2} = 26.46\ Hz$$

For a verification of the result, the shear modulus is calculated with equation (6.2),

$G_{max} = \frac{7000(2.17-e)^2}{1+e}(\sigma'_m)^{0.5}[kN/m^2]$, which is suitable for a gravely silty sand layer. According to (Axelsson & Mattsson, 2016) the porosity for sand and gravel has a value between 15 and 45 percent, and in this case a value between 15 and 25 is reasonable to assume, due to the long term of heavy traffic that this railway has been exposed for. Thus, with a porosity of 20 percent, the pore number is, $e = \frac{n}{1-n} = \frac{0.2}{1-0.2} = 0.25$. Consequently, the shear modulus becomes,

$$G_{max} = \frac{7000(2.17-e)^2}{1+e}(\sigma'_m)^{0.5} = \frac{7000(2.17-0.25)^2}{1+0.25} * (18.81)^{0.5} = 89533\ kN/m^2$$

According to (Angerhn, 2015) the shear wave velocity of gravely sand lies in between 220-450 m/s. By following equation, the shear wave velocity of the subsoil is determined,

$$v_s = \sqrt{G/\rho_w} = \sqrt{91078 * 10^3/2033} = 211.70\ m/s$$

The calculated shear modules correlate well, therefore it is reasonable to assume that the calculation of the subsoils eigenfrequency is acceptable. As well as the shear wave velocity of the gravely silty sand

layer is close to the range of velocities of gravel and sand, an additional confirmation can be performed of the accuracy of the expected eigenfrequencies.

4.2 Expected eigenfrequency of ballast layer

The thickness of the ballast layer is 0.4 meters along Tolikberget, therefore according to Figure 5 should the eigenfrequency for this layer of ballast be quite high. The shear modulus is obtained from (Trafikverket, TK Geo 11, Trafikverkets tekniska krav för geokonstruktioner, Trafikverket, 2011), where the equation is the same as for coarse grained material, namely

$$G_0 = K_1 * (\sigma'_m)^{0.5}$$

Where the constant K_1 for crushed material as ballast is 30000.

The mean effective stress σ'_m is obtained by the relation, $\sigma'_m = \frac{\sigma'_v + \sigma'_h}{2}$. Where

$$\sigma'_v = \gamma'_{Ballast} = 18 * 0.4 = 7.2 \text{ kN}/m^2$$

$$\sigma'_h = K_0 * \sigma'_v = 0.35 * 7.2 = 2.52 \text{ kN}/m^2$$

$$\sigma'_m = \frac{\sigma'_v + \sigma'_h}{2} = \frac{7.2 + 2.52}{2} = 4.86 \text{ kN}/m^2$$

Then the shear modulus becomes

$$G_0 = K_1 * (\sigma'_m)^{0.5} = 30000 * 4.86^{0.5} = 66136.22 \text{ kN}/m^2$$

Consequently, the eigenfrequency of the ballast layer will be

$$f_0 = \frac{v_s}{4H} = \frac{\sqrt{G/\rho}}{4H} = \frac{\sqrt{66136.22 * 10^3/1800}}{4 * 0.4} = 119.80\ Hz$$

Appendix 5 Calculations of expected eigenfrequencies, Polcirkeln-Koskivaara

5.1 Expected eigenfrequency of subsoil

For this case, equation (4.1) is used for calculations of the peat layers eigenfrequency. As the ground water table follows the surface of the swamp, the heaviness of peat must be considered as water saturated. According to (Larsson, 2008) the water saturated heaviness for peat varies between 11 to 13 kN/m^3. Therefore, the water saturated density of peat is at least,

$$\rho_w = \frac{\gamma_w}{g} = \frac{11}{10} = 1.1 \ {}^{t}/_{m^3} = 1100 \ {}^{kg}/_{m^3}$$

And at maximum,

$$\rho_w = \frac{\gamma_w}{g} = \frac{13}{10} = 1.3 \ {}^{t}/_{m^3} = 1300 \ {}^{kg}/_{m^3}$$

According to (Trafikverket, TK Geo 11, Trafikverkets tekniska krav för geokonstruktioner, Trafikverket, 2011) the shear modulus is determined by following relationship,

$$G_0 = 13800 * w_N^{-0.67} * \sigma'^{0.55}_0 \qquad (9)$$

Where, W_N is the water content in peat and σ'_0 is the vertical effective stress. For this case, no reduction of shear modulus is done either, since the initial shear modulus must be used for calculations of the soils eigenfrequency as this is based on the wave velocities. (Studer et.al)

Through investigations the water content is determined for peat in this area, it can vary from 409.5% to 1036.5%. (Gustafsson, Engström, & Finnberg, 2016)

For this case, the water content in the first calculation is chosen to 863.1% and in the second to 409.5%, which are measured values from the investigation.

For calculations of the effective stress, the weight of the ballast and made ground is considered. Consequently, the heaviness for ballast and made ground is obtained from (Larsson, 2008). Which implies that the heaviness for ballast is 18 kN/m^3 and for made ground something between the heaviness for gravel and sand, namely 18.5 kN/m^3. These values are for naturally moisture soil, which is relevant since the soils are above the ground water table. The eigenfrequency calculations are as follows.

Water content 863.1%:

Two calculations of eigenfrequency is performed, one with a density of 1100 ${}^{kg}/_{m^3}$ for peat and another with a density of 1300 ${}^{kg}/_{m^3}$.

Thickness of peat layer 0.7 meters,

The effective stresses, shear modules and eigenfrequencies are as follows:

Density of 1100 $^{kg}/_{m^3}$ for peat,

$\sigma_0' = \gamma'_{Ballast} * z + \gamma'_{Made\ ground} * z + \gamma'_{Peat} * z = (18 * 0.5) + (18.5 * 1.5) + (1 * 0.7) = 37.45\ \mathrm{kN}/m^2$

$G_0 = 13800 * w_N^{-0.67} * \sigma'^{0.55}_0 = 13800 * 8.631^{-0.67} * 37.45^{0.55} = 23884.53\ \mathrm{kN}/m^2$

$f_0 = \frac{v_s}{4H} = \frac{\sqrt{G/\rho_w}}{4H} = \frac{\sqrt{23884.53 * 10^3/1100}}{4 * 0.7} = 52.63\ Hz$

Density of 1300 $^{kg}/_{m^3}$ for peat,

$\sigma_0' = \gamma'_{Ballast} * z + \gamma'_{Made\ ground} * z + \gamma'_{Peat} * z = (18 * 0.5) + (18.5 * 1.5) + (3 * 0.7) = 38.85\ \mathrm{kN}/m^2$

$G_0 = 13800 * w_N^{-0.67} * \sigma'^{0.55}_0 = 13800 * 8.631^{-0.67} * 38.85^{0.55} = 24371.55\ \mathrm{kN}/m^2$

$f_0 = \frac{v_s}{4H} = \frac{\sqrt{G/\rho_w}}{4H} = \frac{\sqrt{24371.55 * 10^3/1300}}{4 * 0.7} = 48.90\ Hz$

Thickness of peat layer 2.5 meters,

The effective stresses, shear modules and eigenfrequencies are as follows:

Density of 1100 $^{kg}/_{m^3}$ for peat,

$\sigma_0' = \gamma'_{Ballast} * z + \gamma'_{Made\ ground} * z + \gamma'_{Peat} * z = (18 * 0.5) + (18.5 * 1.5) + (1 * 2.5) = 39.25\ \mathrm{kN}/m^2$

$G_0 = 13800 * w_N^{-0.67} * \sigma'^{0.55}_0 = 13800 * 8.631^{-0.67} * 39.25^{0.55} = 24509.25\ \mathrm{kN}/m^2$

$f_0 = \frac{v_s}{4H} = \frac{\sqrt{G/\rho_w}}{4H} = \frac{\sqrt{24509.25 * 10^3/1100}}{4 * 2.5} = 14.90\ Hz$

Density of 1300 $^{kg}/_{m^3}$ for peat,

$\sigma_0' = \gamma'_{Ballast} * z + \gamma'_{Made\ ground} * z + \gamma'_{Peat} * z = (18 * 0.5) + (18.5 * 1.5) + (3 * 2.5) = 44.25\ \mathrm{kN}/m^2$

$G_0 = 13800 * w_N^{-0.67} * \sigma'^{0.55}_0 = 13800 * 8.631^{-0.67} * 44.25^{0.55} = 26180 \text{ kN}/m^2$

$f_0 = \frac{v_s}{4H} = \frac{\sqrt{G/\rho_w}}{4H} = \frac{\sqrt{26180*10^3/1300}}{4*2.5} = 14.20\ Hz$

Thickness of peat layer 5.48 meters,

The effective stresses, shear modules and eigenfrequencies are as follows:

Density of 1100 kg/m^3 for peat,

$\sigma'_0 = \gamma'_{Ballast} * z + \gamma'_{Made\ ground} * z + \gamma'_{Peat} * z = (18 * 0.5) + (18.5 * 1.5) + (1 * 5.48) = 42.23 \text{ kN}/m^2$

$G_0 = 13800 * w_N^{-0.67} * \sigma'^{0.55}_0 = 13800 * 8.631^{-0.67} * 42.23^{0.55} = 25515.83 \text{ kN}/m^2$

$f_0 = \frac{v_s}{4H} = \frac{\sqrt{G/\rho_w}}{4H} = \frac{\sqrt{25515.83*10^3/1100}}{4*5.48} = 6.95\ Hz$

Density of 1300 kg/m^3 for peat,

$\sigma'_0 = \gamma'_{Ballast} * z + \gamma'_{Made\ ground} * z + \gamma'_{Peat} * z = (18 * 0.5) + (18.5 * 1.5) + (3 * 5.48) = 53.19 \text{ kN}/m^2$

$G_0 = 13800 * w_N^{-0.67} * \sigma'^{0.55}_0 = 13800 * 8.631^{-0.67} * 53.19^{0.55} = 28968.41 \text{ kN}/m^2$

$f_0 = \frac{v_s}{4H} = \frac{\sqrt{G/\rho_w}}{4H} = \frac{\sqrt{28968.41*10^3/1300}}{4*5.48} = 6.81\ Hz$

Water content 409.5%:

Thickness of peat layer 0.7 meters,

The effective stresses, shear modules and eigenfrequencies are as follows:

Density of 1100 kg/m^3 for peat,

$\sigma'_0 = \gamma'_{Ballast} * z + \gamma'_{Made\ ground} * z + \gamma'_{Peat} * z = (18 * 0.5) + (18.5 * 1.5) + (1 * 0.7) = 37.45 \text{ kN}/m^2$

$G_0 = 13800 * w_N^{-0.67} * \sigma'^{0.55}_0 = 13800 * 4.095^{-0.67} * 37.45^{0.55} = 39361.12 \text{ kN}/m^2$

$$f_0 = \frac{v_s}{4H} = \frac{\sqrt{G/\rho_w}}{4H} = \frac{\sqrt{39361.12*10^3/1100}}{4*0.7} = 67.56\ Hz$$

Density of 1300 kg/m^3 for peat,

$$\sigma_0' = \gamma'_{Ballast} * z + \gamma'_{Made\ ground} * z + \gamma'_{Peat} * z = (18 * 0.5) + (18.5 * 1.5) + (3 * 0.7) = 38.85\ \text{kN}/m^2$$

$$G_0 = 13800 * w_N^{-0.67} * \sigma'^{0.55}_0 = 13800 * 4.095^{-0.67} * 38.85^{0.55} = 40163.73\ \text{kN}/m^2$$

$$f_0 = \frac{v_s}{4H} = \frac{\sqrt{G/\rho_w}}{4H} = \frac{\sqrt{40163.73*10^3/1300}}{4*0.7} = 62.78\ Hz$$

Thickness of peat layer 2.5 meters,

The effective stresses, shear modules and eigenfrequencies are as follows:

Density of 1100 kg/m^3 for peat,

$$\sigma_0' = \gamma'_{Ballast} * z + \gamma'_{Made\ ground} * z + \gamma'_{Peat} * z = (18 * 0.5) + (18.5 * 1.5) + (1 * 2.5) = 39.25\ \text{kN}/m^2$$

$$G_0 = 13800 * w_N^{-0.67} * \sigma'^{0.55}_0 = 13800 * 4.095^{-0.67} * 39.25^{0.55} = 40390.64\ \text{kN}/m^2$$

$$f_0 = \frac{v_s}{4H} = \frac{\sqrt{G/\rho_w}}{4H} = \frac{\sqrt{40390.64*10^3/1100}}{4*2.5} = 19.20\ Hz$$

Density of 1300 kg/m^3 for peat,

$$\sigma_0' = \gamma'_{Ballast} * z + \gamma'_{Made\ ground} * z + \gamma'_{Peat} * z = (18 * 0.5) + (18.5 * 1.5) + (3 * 2.5) = 44.25\ \text{kN}/m^2$$

$$G_0 = 13800 * w_N^{-0.67} * \sigma'^{0.55}_0 = 13800 * 4.095^{-0.67} * 44.25^{0.55} = 43144.09\ \text{kN}/m^2$$

$$f_0 = \frac{v_s}{4H} = \frac{\sqrt{G/\rho_w}}{4H} = \frac{\sqrt{43144.09*10^3/1300}}{4*2.5} = 18.20\ Hz$$

Thickness of peat layer 5.48 meters,

The effective stresses, shear modules and eigenfrequencies are as follows:

Density of 1100 $^{kg}/_{m^3}$ for peat,

$\sigma_0' = \gamma'_{Ballast} * z + \gamma'_{Made\ ground} * z + \gamma'_{Peat} * z = (18 * 0.5) + (18.5 * 1.5) + (1 * 5.48) = 42.23\ \text{kN}/m^2$

$G_0 = 13800 * w_N^{-0.67} * \sigma'^{0.55}_0 = 13800 * 4.095^{-0.67} * 42.23^{0.55} = 42049.47\ \text{kN}/m^2$

$f_0 = \frac{v_s}{4H} = \frac{\sqrt{G/\rho_w}}{4H} = \frac{\sqrt{42049.47*10^3/1100}}{4*5.48} = 8.92\ Hz$

Density of 1300 $^{kg}/_{m^3}$ for peat,

$\sigma_0' = \gamma'_{Ballast} * z + \gamma'_{Made\ ground} * z + \gamma'_{Peat} * z = (18 * 0.5) + (18.5 * 1.5) + (3 * 5.48) = 53.19\ \text{kN}/m^2$

$G_0 = 13800 * w_N^{-0.67} * \sigma'^{0.55}_0 = 13800 * 4.095^{-0.67} * 53.19^{0.55} = 47739.24\ \text{kN}/m^2$

$f_0 = \frac{v_s}{4H} = \frac{\sqrt{G/\rho_w}}{4H} = \frac{\sqrt{47739.24 * 10^3/1300}}{4 * 5.48} = 8.74\ Hz$

5.2 Expected eigenfrequency of ballast layer

The thickness of the ballast layer along Polcirkeln-Koskivaara varies between 0.5 to 1.5 meters, therefore according to Figure 5 should the eigenfrequency of the ballast layer be varying between higher and lower frequencies. The shear modulus is obtained from (Trafikverket, TK Geo 11, Trafikverkets tekniska krav för geokonstruktioner, Trafikverket, 2011), where the equation is the same as for coarse grained material, namely

$G_0 = K_1 * (\sigma_m')^{0.5}$

Where the constant K_1 for crushed material as ballast is 30000.

The mean effective stress σ_m' is obtained by the relation, $\sigma_m' = \frac{\sigma_v' + \sigma_h'}{2}$. Where

A thickness of 0.5 meter ballast gives

$\sigma_v' = \gamma'_{Ballast} = 18 * 0.5 = 9\ \text{kN}/m^2$

$\sigma_h' = K_0 * \sigma_v' = 0.35 * 9 = 3.15\ \text{kN}/m^2$

$\sigma_m' = \frac{\sigma_v' + \sigma_h'}{2} = \frac{9+3.15}{2} = 6.075\ \text{kN}/m^2$

Then the shear modulus becomes

$G_0 = K_1 * (\sigma_m')^{0.5} = 30000 * 6.075^{0.5} = 73942.55\ \text{kN}/m^2$

Consequently, the eigenfrequency of the ballast layer will be

$$f_0 = \frac{v_s}{4H} = \frac{\sqrt{G/\rho}}{4H} = \frac{\sqrt{73942.55*10^3/1800}}{4*0.5} = 101.34\ Hz$$

A thickness of 1.5 meter ballast gives

$$\sigma_v' = \gamma'_{Ballast} = 18 * 1.5 = 27\ \text{kN}/m^2$$

$$\sigma_h' = K_0 * \sigma_v' = 0.35 * 27 = 9.45\ \text{kN}/m^2$$

$$\sigma_m' = \frac{\sigma_v' + \sigma_h'}{2} = \frac{27+9.45}{2} = 18.23\ \text{kN}/m^2$$

Then the shear modulus becomes

$$G_0 = K_1 * (\sigma_m')^{0.5} = 30000 * 18.23^{0.5} = 128089.81\ \text{kN}/m^2$$

Consequently, the eigenfrequency of the ballast layer will be

$$f_0 = \frac{v_s}{4H} = \frac{\sqrt{G/\rho}}{4H} = \frac{\sqrt{128089.81 * 10^3/1800}}{4 * 1.5} = 44.46\ Hz$$